Soft Matter

Accepted Manuscript

ROYAL SOCIETY OF CHEMISTRY

www.rsc.org/softmatter

Critical absorption of a single macromolecule in polymer brushes

Andrey Milchev[1,2], Sergei A. Egorov[3], and Kurt Binder[1]
[1] *Institut für Physik, Johannes Gutenberg-Universität, D-55099 Mainz, Germany,*
[2] *Institute of Physical Chemistry, Bulgarian Academy of Sciences, 1113 Sofia, Bulgaria,*
[3] *Department of Chemistry, University of Virginia, Charlottesville, Virginia 22901, USA*
(Dated: May 21, 2014)

The adsorption of long flexible macromolecules by polymer brush-coated surfaces is studied by Molecular Dynamics simulations and by calculations using density functional and self-consistent field theories. The case of repulsive interactions between the substrate surface and the monomers of both the brush polymers and the extra chains that can get absorbed into the brush is considered. Under good solvent conditions, critical absorption can occur, if the interaction between the monomers of the brush polymers and the extra chain is (weakly) attractive. It is shown that it is possible to map out the details of the critical absorption transition, if the chain length and/or the grafting density of the brush polymers are varied. In this way both the strength and the range of the effective adsorption potential of the substrate surface can be controlled. However, it is found that in the general case there is no straightforward mapping of the present problem to the simpler problem of polymer adsorption in a square well potential, in contrast to suggestions in the literature. In particular, it is found that the fraction of monomers of the long free chain that is absorbed in the brush shows a nonmonotonic variation with the grafting density; i.e. from dense brushes free chains again are expelled from their interior. For strong enough attraction the free chain then gets adsorbed at the brush - solution interface.

I. INTRODUCTION

The adsorption transition of a single long flexible macromolecule from dilute solution under good solvent conditions exposed to an attracting surface has found abiding interest in the literature (see e.g. [1–21]). As long as the macromolecule is not adsorbed, it forms a swollen coil in the solution, characterized by the famous Flory relation for the gyration radius R_g considered as a function of the "chain length" N (i.e., number of monomeric units forming the polymer), $R_g \propto N^{\nu}$, with $\nu = 3/5$ (according to Flory [22, 23]) or $\nu \approx 0.588$ (according to renormalization group theory [24] and extensive Monte Carlo simulations [25, 26]). At the adsorption transition, the entropic repulsion of the surface (the chain has less configurations when it is attached to the substrate) is overcome by the enthalpic binding to the substrate, ultimately the adsorbed chain resembles a self-avoiding walk in $d = 2$ space dimensions ($R_g^{ads} \propto N^{\nu_2}$ with [23] $\nu_2 = 3/4$). The crossover between these two limiting behaviors has been a delicate theoretical problem [1, 7, 11–19] and the details of this behavior are heavily debated until today [19, 20].

However, although the problem of polymer adsorption on surfaces is relevant in many contexts (biomolecules interacting with cell surfaces, control of nanocrystal growth by adsorbed polymers, fabrication of special polymeric coatings at substrates, etc.), the experimental studies which could elucidate the detailed properties of polymers when they undergo critical adsorption still remain to be performed! In fact, it is not at all straightforward in an experiment to vary the adsorption potential that monomers experience at a surface, without changing the solvent quality of the bulk solution.

Of course, it is possible (and this can be useful for applications) to modify the adsorption potential (i.e., its strength, its range, or both) of a surface acting on macromolecules by adsorbing a suitable species of small molecules at the surface, which then may "screen" somewhat the substrate from the adsorbing polymer. However, in such a case one does not know in full detail the resulting total effective potential that the monomers of the adsorbing long macromolecule experience. E.g., varying the concentration of this surface-active small molecules in the solution may lead to a rather nonlinear response of this effective potential, depending on the structure and thickness of the small molecule layer bound to the surface. Understanding such phenomena in full atomistic detail is a formidable problem, and requires to consider the detailed chemistry of the system, which is out of our scope here, where we focus on generic aspects of the adsorption transition.

At this point we also mention the relation of the problem studied in our paper to Reversed Phase Liquid Chromatography (RPLC) [27–33]. This is one of the main methods to separate macromolecules in solution, and typically it uses a silica surface to which short alkyl chains (typically not more than 30 carbon atoms long) are rather densely grafted [33]. These "hairy" surfaces then may be very efficient in the retention of macromolecules from the solution, and clearly it is very important to understand how the structure of this dense layer of short grafted chain molecules controls the efficiency of adsorption of long macromolecules. Although alkyl chains have a significant intrinsic chain stiffness, it is widely accepted that one should describe them in their state at "hairy" surfaces not like rigid rods. They still have some flexibility [32], albeit they resemble a "polymer bristle" [34] rather than standard polymer brushes where the concentration of monomers in most cases is in the semidilute concentration regime [35, 36]. We note that for chromatography applications it is necessary either to adjust the temperature or the solvent composition such that one is close to the critical conditions for polymer adsorption (otherwise chains are irreversibly adsorbed in the brush, or nothing is adsorbed). While the application of the adsorption of long macromolecules by polymer brushes for RPLC is not our focus, we draw attention to the fact that our study may be useful in this context.

The purpose of the present work is to demonstrate by both computer simulations and accompanying theory that a lot of insight on the adsorption of polymers on surfaces can be gained when one considers the related problem of adsorption of very long macromolecules in a polymer brush [37], if the brush height h satisfies the condition $h \ll R_g$ (of the free chains). Thus, the chains in the brush must have a chain length $N_g \ll N_f$, of course, but varying either

N_g or the grafting density σ_g (or both), it becomes possible to scan the transition from the desorbed to the adsorbed state of the long flexible polymer. However, we shall demonstrate that one must distinguish between absorption of a chain inside a brush and adsorption on the brush-solution interface.

The outline of this paper is as follows. In Section II, the main theoretical predictions about the adsorption transition of polymers are summarized. Section III describes the model used in the simulation, while Section IV describes our simulation results. Section V presents our calculations based on density functional theory and self-consistent field theory, and Section VI summarizes our conclusions.

II. THEORETICAL BACKGROUND

A. Scaling Description of the Adsorption Transition

The qualitative picture of an adsorbed chain close to the adsorption transition is a chain of "blobs" of diameter ξ, whereby each blob contains $g \gg 1$ monomers of the chain under good solvent conditions, and the structure of the chain inside a blob follows the statistics of polymer coils in (bulk) three-dimensional polymer solutions, i.e. $\xi = ag^{\nu}$, where a is the size of an effective monomeric unit (here and in what follows prefactors of order unity will be systematically suppressed). The blobs are self-avoiding as well and form a structure of a two-dimensional self-avoiding walk on the surface, of radius R_{xy} (we orient the coordinate system such that the x, y axes are parallel to the substrate and the z-axis is perpendicular to it) given by $R_{xy} = \xi n_b^{\nu_2}$ where $n_b = N/g$ is the number of blobs. Since $g = (\xi/a)^{1/\nu}$, this yields

$$R_{xy} = a(\xi/a)^{1-\nu_2/\nu} N^{\nu_2} \tag{1}$$

The adsorbed chain is sometimes described as a "pancake" of thickness ξ, but one must realize that this "pancake" is not compact, since the average density ρ of the "pancake" is of order

$$\rho = N/(R_{xy}^2 \xi) = N^{1-2\nu_2}(\xi/a)^{(2\nu_2/\nu-3)} a^{-3} \approx N^{-1/2} a^{-3} (\xi/a)^{-1/2} \tag{2}$$

In the last step, the Flory approximation ($\nu \approx 3/5$) was invoked. Note that when one approaches the adsorption transition, ξ grows up to the size of a "mushroom" (a chain anchoring with one end at the substrate but otherwise being repelled by the surface) $R_{xy}^{mush} = R_z^{mush} = aN^{\nu}$, with $n_b = 1$. Obviously, then a smooth crossover of the linear dimensions of the pancake to the linear dimensions of the mushroom occurs, and also the density of the "pancake" has decreased from its value of a strongly adsorbed chain ($\rho = a^{-3}N^{-1/2}$) to the density of the mushroom ($\rho^{mush} = a^{-3}N^{1-3\nu} \approx a^{-3}N^{-4/5}$).

The free energy (in units of k_BT) is written as a sum of a repulsive term (which can be interpreted by the number of blobs in the pancake) and an attractive term. The latter is proportional to the temperature distance from the adsorption transition temperature T_a, and the number of monomer-surface contacts which is written as $n_b g^{\phi}$, where ϕ is the so-called "crossover exponent". At T_a, this number of monomer-surface contacts (or number of adsorbed monomers, respectively) is simply $N_s \propto N^{\phi}$. Thus

$$F = F_{\rm rep} + F_{\rm attr} = N(\xi/a)^{-1/\nu} - cNt\Big(\xi/a\Big)^{(\phi-1)/\nu} \quad , \tag{3}$$

where we have defined $t = T_a/T - 1$.

In the spirit of Flory's arguments, one minimizes F with respect to ξ to clarify the temperature dependence of ξ. From $(\partial F/\partial \xi)_{N,T} = 0$ one finds

$$(\xi/a) \propto t^{-\nu/\phi} \quad , \quad N \to \infty \quad . \tag{4}$$

The divergence of ξ as $T \to T_a$ is rounded off, of course, when ξ becomes of the order of $R_z^{\rm mush}$. Only when we take the thermodynamic limit $N \to \infty$ first, and then consider the limit $T \to T_a$, is the adsorption transition a sharp transition. The adsorbance (fraction of adsorbed monomers) simply is

$$\frac{N_s}{N} = f_s = ct^{\frac{1-\phi}{\phi}} \quad , \quad N \to \infty \quad , \tag{5}$$

but also the vanishing of f_s as $T \to T_a$ is rounded off when N is finite by the finite size effect of the chain.

In simple mean-field theories of the adsorption transition [38] where one assumes ideal chains for which $\nu = 1/2$ (and also $\phi = 1/2$), both the inverse thickness of the adsorbed "pancake" and the adsorbance vary linearly with inverse temperature, $\frac{a}{\xi} \propto \frac{N_s}{N} \propto t$. While Gorbunov and Skvortsov [38] argue that the existing experimental data are compatible with this relation for the adsorption correlation length ξ, we feel that more precise measurements are needed to characterize quantitatively the critical behavior near the transition. The situation is reminiscent of the early days of research on magnetism when data on the temperature dependence of the spontaneous magnetization were fitted to the Weiss molecular field theory. We also remark that it is difficult to measure the adsorption correlation length ξ directly by means of scattering methods. Frequently it is estimated indirectly using chromatography data on partition coefficients [38]. As far as $\nu(\approx 3/5)$ differs appreciably from $\phi(\approx 1/2)$, there is some non-linearity in the

relation between (a/ξ) and t albeit this non-linearity is not as strong as was erroneously assumed originally, (taking $\phi = 1 - \nu \approx 2/5$) [5].

These crossovers from the "pancake" to the "mushroom" behavior can be described formally in terms of crossover scaling functions $\tilde{R}_{gxy}$, $\tilde{R}_{gz}$ for the components of the gyration radius of the chain, e.g.

$$R_{gz}/a = N^{\nu}\ \tilde{R}_{gz}\{tN^{\phi}\} \quad , \tag{6}$$

and similarly for the adsorbance $\{\tilde{N}(\varsigma)$ with $\varsigma = tN^{\phi}$, being one more crossover scaling function$\}$

$$N_s/N = N^{\phi-1}\ \tilde{N}\{tN^{\phi}\} \quad . \tag{7}$$

The scaling function $\tilde{N}$ has a nontrivial limiting behavior for $T > T_a$, since the fact that only few monomers are adsorbed implies that $N_s/N \propto 1/N$ in this limit, which requires that

$$\tilde{N}(\varsigma) \propto \varsigma^{-1} \quad , \quad \varsigma \to -\infty \quad . \tag{8}$$

For $\varsigma \to +\infty$, the asymptotic behavior of the scaling functions in Eqs. (6), (7) is

$$\begin{aligned} \tilde{R}_{gz}(\varsigma) &\propto \varsigma^{-\nu/\phi} \\ \tilde{N}(\varsigma) &\propto \varsigma^{(1-\phi)/\phi}, \end{aligned} \tag{9}$$

However, both the prediction for ϕ, and the explicit computation of the scaling functions defined above, is a highly nontrivial task for renormalization group methods [1] as well as for Monte Carlo simulations [7, 13, 15, 16, 20].

B. Effects of the variation of the range of the adsorption potential

Consistent with early studies of the problem [1–19], we have addressed so far only the case of an extremely short range adsorption potential (the range of the potential being of the same order as the monomer linear dimension a). Only recently, a systematic study was presented [20] in order to clarify how the range of the adsorption potential affects the location of the adsorption transition. For simplicity, a square well potential was assumed [20]:

$$V(z) = \begin{cases} \infty, & z < 0 \\ -U, & 0 < z \le W \\ 0, & z > W \end{cases} \quad , \tag{10}$$

so U is the strength, and W, the range of this potential.

Although mean field theory (which implies $\nu = \nu_2 = \phi = 1/2$) cannot meaningfully address the crossover described by Eqs. (6-9), the question of finding the location of the adsorption transition for this potential can already be addressed in mean field theory, where the excluded volume interaction is neglected [20]. In the continuum approximation, the Green's function of the chain (describing the partition function of the chain keeping its end at fixed positions) satisfies a differential equation analogous to the Schrödinger equation [1]. Exploiting the quantum mechanical analogy, the adsorbed state corresponds to the bound state of a quantum particle in this potential, which exists only for $U > U_c$ with [20]

$$U_c = a^2\pi^2/(24W^2) \quad . \tag{11}$$

It can be shown [20, 37], that the adsorbed fraction θ of monomers (i.e., the monomers with z-coordinates $z \le W$) is given by

$$\theta(u) \approx u \quad , \quad u \ll 1 \tag{12}$$

$$\theta(u) \approx 1 - \frac{5}{2}(u+1)^{-3/2} \quad , \quad u \gg 1, \tag{13}$$

where the parameter u is defined by $u = U/U_c - 1$.

Of course, the linear variation of the adsorbed fraction θ is in agreement with Eq. (5), if there the mean field value $\phi = 1/2$ for the crossover exponent [1, 7] is used.

For self-avoiding walks (SAWs) on the simple cubic lattice the adsorption potential, Eq. (10), was studied by extensive Monte Carlo simulations [20] using the pruned enriched Rosenbluth method (PERM) [39, 40]. The result could be cast in the form

$$U_c = \frac{0.585}{(W+1/2)^{5/3}}\ , \tag{14}$$

where the exponent 5/3 should simply be interpreted as $1/\nu$ (note that in mean field $\nu = 1/2$ and then the exponent 2 of Eq. (11) results). In fact, for the potential, Eq. (10), a fully adsorbed chain will not be a strictly two dimensional SAW (like considered in Section II A) but rather a two-dimensional chain of blobs of diameter W. Each blob contains $g = (W/a)^{1/\nu}$ segments ($W = ag^{\nu}$, cf. Section II A). Then the total energy of a blob is of order $gU = (W/a)^{1/\nu}U$. The adsorption transition must occur when this energy (in units of k_BT) is of order unity [20], yielding $U_c \propto W^{-5/3}$, qualitatively compatible with Eq. (14). The Monte Carlo simulations [20] suggested that the crossover exponent $\phi \approx 0.48$, compatible with the previous estimation (for $W = 1$) from Grassberger [16], and independent of W, as expected from the universality principle of renormalization group theory [1, 11, 41].

C. Absorption of a Chain in a Polymer Brush: Theoretical Considerations

Skvortsov et al. recently suggested [37] that in practice an adsorption potential with a large but finite range "W" could be physically realized via the absorption of a long chain from dilute solution in a polymer brush with weakly attractive interaction between the brush monomers and the monomers of the extra chain. In the following, we briefly examine and extend this argument.

Polymer brushes are formed by grafting chains (we consider a monodisperse brush with chains of length N_g) at a flat planar substrate with one of their chain ends at grafting density σ_g. The theory of polymer brushes has been studied extensively for a long time [35, 36]. Here we deal with polymer brushes on the level of the simple Alexander [42]-de Gennes [43] model, which assumes a constant density of the monomers of the chains in the brush up to the brush height h, and zero monomer density for $z > h$. Good solvent conditions for the brush chains and repulsive interactions between all monomers and the planar substrate surface are assumed.

The scaling theory [42, 43] is then again formulated in terms of a blob picture: each chain is essentially confined into a cylinder of diameter $\sigma_g^{-1/2}$, the axis of the cylinder is oriented perpendicular to the substrate. The overall monomer density in the brush should be in the semi-dilute [23] regime, i.e., $\sigma_g^{-1/2} \gg a$, and hence one can apply again SAW statistics inside the blob, which means that each blob contains g monomers, with $\sigma_g^{-1/2} = ag^{\nu}$, $g = (\sigma_g a^2)^{-1/(2\nu)}$, and the number n_b of blobs in one such cylindrical string is $n_b = N_g/g = (\sigma_g a^2)^{1/(2\nu)}N_g$. The brush height then is [42, 43]

$$h/a = (\sigma_g a^2)^{-1/2} n_b = (\sigma_g a^2)^{\frac{1}{2}(\frac{1}{\nu}-1)} N_g \approx (\sigma_g a^2)^{1/3} N_g \quad . \tag{15}$$

The free energy per chain again is just the number of blobs

$$F_{\rm chain} = n_b = (\sigma_g a^2)^{1/(2\nu)} N_g \quad , \tag{16}$$

and the monomer density in the brush is

$$\rho_{\rm brush} a^3 = g/(\sigma_g a^2)^{-3/2} = (\sigma_g a^2)^{(3-\frac{1}{\nu})/2} \approx (\sigma_g a)^{2/3} \tag{17}$$

The assumption proposed by Skvortsov et al. [37] now is that in the semidilute limit where $\rho_{\rm brush} a^3 \ll 1$, the effect of an extra chain with N_f monomers, that is absorbed in the brush, on the brush structure itself can be completely neglected. Then, one could describe the interaction of the brush monomers with those of the extra chain by a uniform potential, namely Eq. (10), with [37]

$$W = h, \quad U = \varepsilon_{fg}\, \rho_{\rm brush} a^3, \quad F \propto -N_f u^{1+(1-\phi)/\phi} \tag{18}$$

where ε_{fg} is the absolute value of the effective attractive energy acting between the monomers of the free chain and the grafted chains, and Eqs. (3), (4) were invoked, and $U_c(W)$ is given by Eq. (11). Consistency with the mean-field description of Eqs. (11)-(13) implies to take also $\phi = 1/2$, of course, and so the free energy of an extra chain $F \propto N_f u^2$.

An alternative treatment of the problem can be based on the Flory approach [22, 23, 44]. The free energy of a brush composed of G chains grafted on the area A (so that $\sigma_g = G/A$) is written as a sum of two terms, an elastic contribution (cost of stretching the "entropic springs") so that the chains have an end-to-end distance h rather than $a\sqrt{N_g}$) and the repulsive energy (due to excluded volume interactions between the monomers of the grafted chains). This latter energy density per unit volume is written as $v_2 a^3 \rho_{\rm brush}^2$, where v_2 is the second virial coefficient. Since $\rho_{\rm brush} = GN_g/(Ah)$, we find

$$F = F_{\rm chain} G = Gh^2/(N_g a^2) + v_2 a^3 (GN_g)^2/(Ah) \tag{19}$$

Minimizing F with respect to h yields

$$h/a = (v_2/2)^{1/3}\ (\sigma_g a^2)^{1/3}\ N_g \tag{20}$$

compatible with Eq. (15). However, the situation is somewhat subtle, since the corresponding free energy of a chain in the brush

$$F_{\rm chain} = 3\Big(\frac{v_2}{2}\Big)^{2/3}\Big(\sigma_g a^2\Big)^{2/3} N_g \tag{21}$$

exhibits a scaling power of σ_g (namely 2/3) which differs from the blob prediction (Eq. (16) suggests $\sigma_g^{1/(2\nu)} \approx \sigma_g^{5/6}$). Such discrepancies between scaling descriptions based on the blob concept and the Flory approach are familiar from other contexts, e.g. linear polymers and star polymers under confinement [45].

Notwithstanding such problems, we try an extension of Flory theory to the case when a free chain is incorporated into the brush, replacing Eq. (19) with the help of Eq. (18) by (recall $U = \epsilon_{fg} a^3 \rho_{brush} = \epsilon_{fg} a^3 G N_g/(Ah)$ and $U_c = a^2\pi^2/24h^2$)

$$F = \frac{Gh^2}{a^2 N_g} + v_2 a^3 \frac{(GN_g)^2}{Ah - N_f a^3} - cN_f \Big(\frac{24}{\pi^2} \frac{haN_g G \varepsilon_{fg}}{A} - 1 \Big)^2 \quad . \tag{22}$$

Here we have accounted for the fact, that the volume V taken by the brush monomers is no longer Ah but reduced to $Ah - N_f a^3$, taking into account the volume of all the monomers of the extra chain when it is fully absorbed into the brush. For the free energy of adsorption of the extra chain we have taken the last expression of Eq. (18), using $\phi = 1/2$ for simplicity, and using $U_c(W) = U_c(h)$ according to Eq. (11), and c is a constant. Minimizing Eq. (22) with respect to h, one finds that the absorption of the extra chain leads to a swelling of the brush (over the area A taken by the projection of the extra chain to the grafting surface), namely $h = h_0(1 + \Delta)$ where h_0 is the result written in Eq. (20). We expand the equation $\partial F/\partial h = 0$ in leading order in both Δ and $N_f a^3/(Ah_0)$, to find after some algebra that for very large N_f the relative change of the brush height Δ is given by

$$\Delta \approx \frac{1}{3} \frac{N_f a^3}{Ah_0} \Big\{ 2 + c \frac{U}{U_c} u \Big(\frac{v_2}{2} \Big)^{-1/3} \Big(\sigma_g a^2 \Big)^{-4/3} \Big\} \quad . \tag{23}$$

For self-consistency, A needs to be taken as $\pi R_{||}^2(N_f)$, with $R_{||} \approx h_0 n_b^{3/4}$, describing the absorbed chain as a two-dimensional self-avoiding walk of blobs of diameter h_0, the number of blobs being $n_b = N_f/g$ where $g = (h_0/a)^{5/3}$, i.e., $R_{||} \approx a(h_0/a)^{-1/4} N_f^{3/4}$. Thus, the prefactor of the curly bracket scales as $\propto \sqrt{a/h_0 N_f}$, that is, $N_f a^3/(Ah_0) \propto N_f a^3/(a^{5/2} h_0^{1/2} N_f^{3/2}) = \sqrt{a/(h_0 N_f)}$, if $n_b \gg 1$. We also note that the swelling increases linearly with the relative distance u from the adsorption transition. Of course, the assumptions made are applicable only if the extra chain is fully absorbed in the brush. For a truly self-consistent treatment numerical calculations based on the self-consistent field theory [2], or computer simulations, are required. Note also that Eqs. (22), (23) can only describe the problem qualitatively for the semidilute limit. Eq. (22) expresses the critical value of the adsorption energy ε_{fg} as

$$\varepsilon_{fg}^c = \frac{\pi^2}{24 (v_2/2)^{2/3} (\sigma_g a^2)^{4/3} N_g^2} \tag{24}$$

This expression clearly demonstrates again that in this problem the adsorption transition can be controlled either by variation of the energy strength ε_{fg} or of the grafting density σ_g or the chain length N_g of the grafted chains. It must be emphasized, however, that all relations of this subsection are only valid for very large N_f, namely the extra chain must be so long that its radius R in bulk solution by far exceeds the brush height, $R \gg h$.

It is instructive to consider also the opposite limit, $R \ll h$. Since the free chain in bulk solution is our reference state for the free energy of the extra chain, the free energy of the absorbed chain in the brush is no longer given by the last term on the right hand side of Eq. (22), but simply by the adsorption enthalpy ($-UN_f = -\varepsilon_{fg}\, N_f \rho_{\rm brush} a^3$, cf. Eq. (18)), when we neglect the translational entropy of localizing the free chain in the region $0 < z < h$. In simulations or numerical self-consistent field calculations, where a finite linear dimension L_z of the system in z-direction is used, this entropy would be $\ln(L_z/h)$, but it does not play a role in a real system apart from controlling the fraction of adsorbed chains relative to the non-adsorbed chains in the bulk solution. In any case, there is no longer a change of configurational entropy of the chain upon absorption, unlike for the limit $R \gg h$. This adsorption enthalpy then competes with the free energy cost of swelling the brush due to absorption, as contained in the second term on the right hand side of Eq. (22). To leading order the sum of these two terms is, normalized per chain in the brush

$$\Delta F = v_2 a^3 \frac{GN_g^2}{Ah} \frac{a^3 N_f}{Ah} - \frac{\varepsilon_{fg} N_g N_f a^3}{Ah} \quad . \tag{25}$$

One sees that the condition $\Delta F = 0$ leads to the condition

$$\varepsilon_{fg}^{\rm c} = v_2 a^3 \frac{GN_g}{Ah} = v_2 a^3 \rho_{\rm brush} \quad . \tag{26}$$

Thus, there exists a linear scaling of the critical strength of the energy $\varepsilon_{fg}^{\rm c}$ with the monomer density $\rho_{\rm brush}$ in the polymer brush. Such a critical value would be absent for adsorption in a single square well potential, of course. Absorption of short chains in brushes has been studied by us in earlier work [46] and thus is not our main focus here, however.

As a final caveat of this section, we mention that in our estimate for U_c in Eqs. (22), (24) we have simply used the relation Eq. (11) instead of Eq. (14), hence ignoring excluded volume between the monomers of the adsorbed chain inside the brush. We also have not considered the effect that for partially absorbed chains the parts of the chain that are still outside of the brush experience a full excluded volume interaction, while the latter is to some extent screened for the parts of the chain inside the brush. However, both MD (Section IV) and SCFT (Section V) would account for such effects.

III. MODEL DESCRIPTION

We consider a coarse-grained model [47] of a polymer brush which consists of linear flexible chains of length N_f with one end free and the other one tethered on a square lattice of size $L_{xy} = 50\sigma$. Typically, grafting densities in the range $0.0625 \leq \sigma_g \leq 0.25$ have been studied.

The bonded interaction between subsequent beads is described by the frequently used Kremer-Grest potential [48] $V^{\rm KG}(r) = V^{\rm FENE} + V^{\rm WCA}$, with the so-called 'finitely-extensible nonlinear elastic' (FENE) potential:

$$V^{\rm FENE}(r) = -0.5kr_0^2 \ln\left[1 - (r/r_0)^2\right] \tag{27}$$

The non-bonded interactions between monomers are taken into account by means of the Weeks-Chandler-Anderson (WCA) interaction, i.e., the shifted and truncated repulsive branch of the Lennard-Jones potential given by:

$$V^{\rm WCA}(r) = 4\epsilon\left[(\sigma/r)^{12} - (\sigma/r)^6 + 1/4\right]\Theta(2^{1/6}\sigma - r) \tag{28}$$

which describes the case of good solvent conditions. In Eqs. (27) and (28), r denotes the distance between the center of two monomers (beads), while the energy scale ϵ and the length scale σ are chosen as the units of energy and length, respectively. Accordingly, the remaining parameters are fixed at the values $k = 30\epsilon/\sigma^2$, $r_0 = 1.5\sigma$. In Eq. (28) we have introduced the Heaviside step function $\Theta(x) = 0$ or 1 for $x < 0$ or $x \geq 0$. With these parameters the typical bond length is $b \approx 0.967\sigma$. Since we have chosen $\sigma = 1$, the bond length is of order unity as well, and also the thermal energy $k_BT = 1$.

The non-bonded interaction between the polymer brush and the adsorbing single chain was described by the full Lennard-Jones potential without truncation, cf. Eq. (28), and characterized by strength $\epsilon = \epsilon_{fg}$, which in our simulations varies typically within the interval $0.1 \leq \epsilon_{fg} \leq 0.6$. We sample the components of the mean squared radius of gyration, $R^2_{g||}$, $R^2_{g\perp}$ and end-to-end distance, $R^2_{e||}$, $R^2_{e\perp}$ of the adsorbing chain parallel and normal to the grafting plane as well as the internal energy U (per monomer). Another important quantity that is indicative for the onset of polymer adsorption in the brush coating is the *adsorbance* (i.e., adsorbed amount) $\Gamma_{ads}(\epsilon_{fg})$ which describes the fraction of chain monomers residing between the grafting surface and a distance z_h that contains 99% of the monomers belonging to the polymer brush.

The equilibrium dynamics of the chain is obtained by solving the Langevin equation of motion for the position $\mathbf{r}_n = [x_n, y_n, z_n]$ of each bead in the chains,

$$m\ddot{\mathbf{r}}_n = \mathbf{F}_n^{\rm FENE} + \mathbf{F}_n^C - \gamma\dot{\mathbf{r}}_n + \mathbf{R}_n(t), \tag{29}$$

which describes the Brownian motion of a set of interacting monomers. In Eq. (29) $\mathbf{F}_n^{\rm FENE}$ and $\mathbf{F}_n^C$ are deterministic forces exerted on monomer n by the remaining bonded and nonbonded monomers, respectively. While for bonded monomers, or pairs of monomers belonging to the polymer brush, or to the free chain, the conservative forces are purely repulsive, $\mathbf{F}_n^C = \nabla V^{WCA}(r)$, the forces between free chain- and brush segments correspond to attractive Lennard-Jones interactions, $\mathbf{F}_n^C = \nabla V^{LJ}(r)$, with amplitude $\epsilon = \epsilon_{fg}$.

The influence of solvent is split into a slowly evolving viscous force $-\gamma\dot{\mathbf{r}}_n$ and a rapidly fluctuating stochastic force $\mathbf{R}_n$. The random, Gaussian force $\mathbf{R}_n$ is related to the friction coefficient γ by the fluctuation-dissipation theorem. The integration step was 0.002 time units (t.u.) and time is measured in units of $\sqrt{m\sigma^2/\epsilon}$, where m denotes the mass of the beads, $m = 1$. The ratio of the inertial forces over the friction forces in Eq. (29) is characterized by the Reynolds number $\mathrm{Re} = \sqrt{m\epsilon}/\gamma\sigma$ which in our setup is $\mathrm{Re} = 4$. In the course of our simulations the velocity-Verlet algorithm was employed to integrate equations of motion (29).

A subtle problem is the proper choice of the linear dimensions $L_x = L_y$ and L_z of the simulation box. Since in the lateral xy-directions periodic boundary conditions (*pbc*) are used, L_x has to be chosen large enough so that the configuration of the chain that gets absorbed in the brush (or adsorbed on the brush-solution interface) is not constrained by interactions of monomers in the basic simulation box with its images created by the *pbc*. Using $N_f = 100$ to $N_f = 600$ we find that $\langle R_g^2\rangle$ in the solution varies from about roughly 30 to roughly 150, leading to typical end-to-end distances in the range from 13 to 30. Of course, an adsorbed chain that satisfies two-dimensional self-avoiding walks statistics can have significantly larger parallel components of its end-to-end distance, so it would be desirable to choose L_x very large. On the other hand, most of the computational effort of the MD code inevitably is spent on updating the positions of the brush monomers, and choosing L_x very large means a waste of computational resources. As a consequence of these conflicting considerations we have chosen $L_x = 40$ or $L_x = 50$ as a compromise.

Also the choice of L_z requires care: to localize the non-adsorbed chain in the simulation box, we choose $L_z = 60$, and take also a repulsive wall potential at $z = L_z$, using the same form as Eq. (28). Note that in the ideal case one would have to simulate a macroscopically large system containing a dilute solution of the free chains interacting with the brush-coated wall. This is not possible and so one simulates a single free chain interacting with the brush. As is well known, the free chain then has a translational entropy $S_{trans} = \ln(L_z/const.)$, and so the thermodynamic limit $L_z \to \infty$ cannot be taken. In fact, for rather small N_f this term leads to appreciable L_z-dependence of physical observables. To avoid this problem, it is customary to localize the chain, e.g., by end-grafting it at the surface. Actually, the standard setup for simulation of polymer adsorption hence is the study of adsorption of such a "polymer mushroom" [7–10, 13, 15–21]. This is not done here because a number of monomers near the grafting site would then always strongly interact with the brush, and hence the fraction of monomers absorbed in the brush would be distinctly non-zero also for non-adsorbed polymers, far away from the adsorption transition. So we decided to localize the non-adsorbed chain in the region above the brush by choosing $L_z - h$ (typical values of the brush heights h are

in the range from 10 to 25, for our choices of parameters) similar to L_x which was the motivation for the arbitrary choice $L_z = 60$ quoted above. One must accept that the "finite-size effects" on the adsorption transition due to the finiteness of N_f depend somewhat on this choice (and differ from those for the adsorption of mushrooms), however.

IV. SIMULATION RESULTS

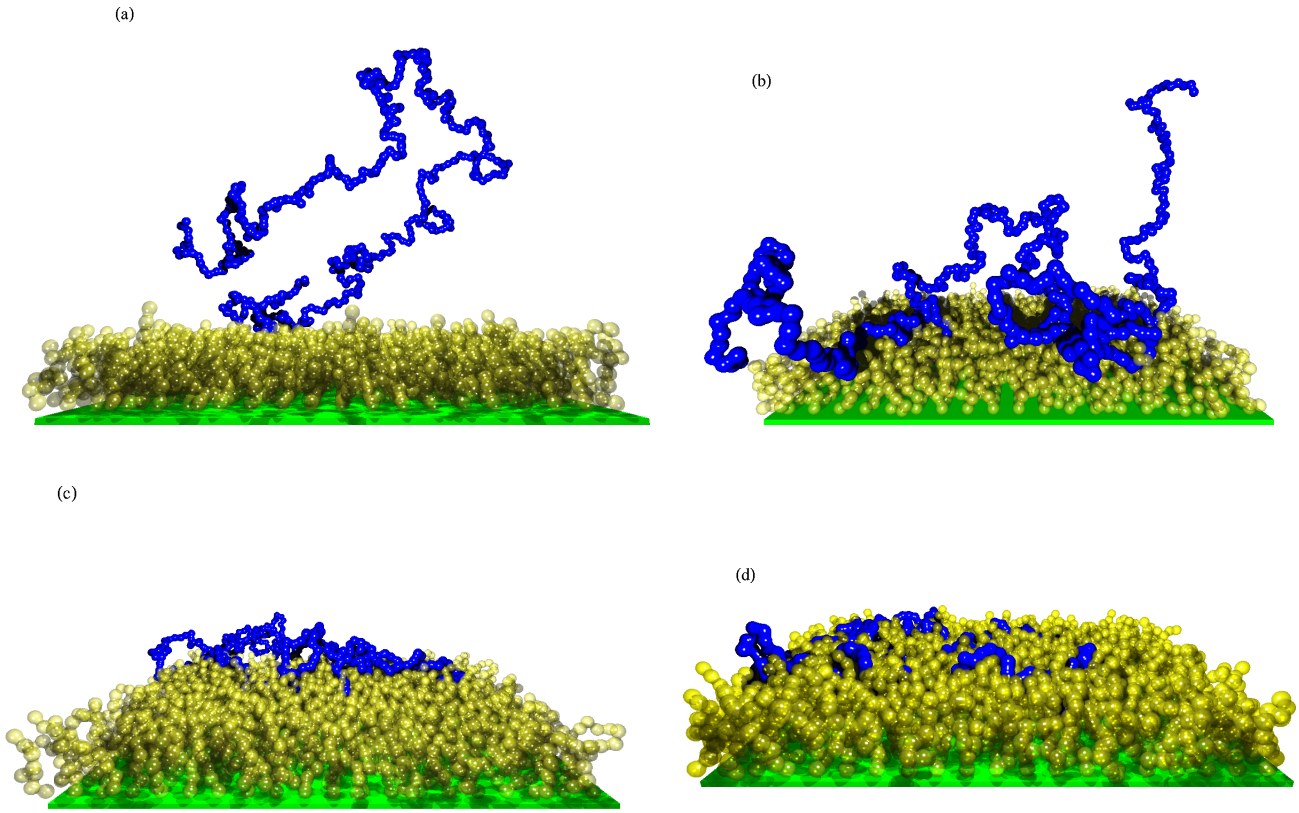

FIG. 1: Snapshots of a single polymer chain with length $N_f = 400$ in a polymer brush at grafting density $\sigma_g = 0.25$. The polymer brush is made of $N_{ch} = 625$ chains of length $N_g = 16$, and has lateral dimension 50×50. The strength of the brush - polymer interactions ϵ_{fg} is taken as: (a) $\epsilon_{fg} = 0.34$, (b) $\epsilon_{fg} = 0.38$, (c) $\epsilon_{fg} = 0.46$, and (d) $\epsilon_{fg} = 0.58$.

Fig. 1 presents a series of simulation snapshots for the typical choice of parameters that is accessible in the simulation, namely $N_f = 400$, $N_g = 16$ and $\sigma_g = 0.25$. Varying the strength of the interaction ε_{fg} between the monomers of the free chain and the monomers of the grafted chains forming the brush, one sees that indeed several distinct cases occur: for $\varepsilon_{fg} = 0.34$ (Fig. 1a) the free chain still is completely outside of the brush, the favorable binding energy that the monomers of the free chain could win in the brush cannot compensate for all the losses of entropy, due to the strongly reduced number of configurations accessible to the free chain, and additional elastic energy occurring for chains of the brush, when a free chain is incorporated into the brush, necessitating additional stretching of the brush chains. However, a relatively small increment of this binding enthalpy (from 0.34 to 0.38) suffices to adsorb the chain at the brush-solution interface (Fig. 1b). In this state, there still occur large "loops" and one long "tail" of the adsorbed chain that reach far out into the region of the solution. Although the lateral linear dimension of the adsorbed chain now is somewhat larger than the perpendicular one, unlike the case Fig. 1a, this increase of the linear dimension is not yet dramatic, so we have found a state that is still close to the adsorption transition. However, for $\varepsilon_{fg} = 0.46$ (Fig. 1c), the situation is very different: only small loops occur by which the free chain can still make "excursions" into the solution above the brush, and most of the monomers of the free chain have been "sucked in" deeply into the brush, and therefore are not seen in the snapshot any longer. The perpendicular linear dimension R_{gz} of the absorbed extra chain has a value that is close to the height of the brush. If one increases ε_{fg} further (Fig. 1d), the picture does not change much: the loops of the absorbed chains that still stick out of the brush have become a bit smaller.

Of course, the snapshots also demonstrate the type of compromises that need to be made in simulations to test the theory: the rather large grafting density chosen clearly has the effect that the monomer density inside the brush corresponds to a rather concentrated solution, instead of the semidilute solution addressed in the theories. This rather large grafting density was necessary to achieve a reasonably strong stretching of the brush chains, for the rather short chain length $N_g = 16$ that was chosen. Although the chain length N_f of the free chain exceeds N_g by a factor 25, the

linear dimension of the free chain in solution (R) exceeds the brush height h only by a factor of order $3-5$. Thus, the theoretical limit $R \gg h$ has been reached, but the price to be paid is that we had to consider a rather dense brush of fairly short chains. Therefore, it is no surprise that a relatively large energy $\varepsilon_{fg}(\varepsilon_{fg} \cong 0.4)$ is needed to absorb the chain into the brush. But similar caveats need to be made about possible experiments: the joint limits to be taken in the theory outlined in Section II ($\sigma_g \to 0$ and $N_g \to \infty$ such that the number of blobs $n_b \gg 1$, and $N_f \to \infty$ such that $R \gg h$ still is realized) is clearly elusive to simulations, but also barely accessible in experiment.

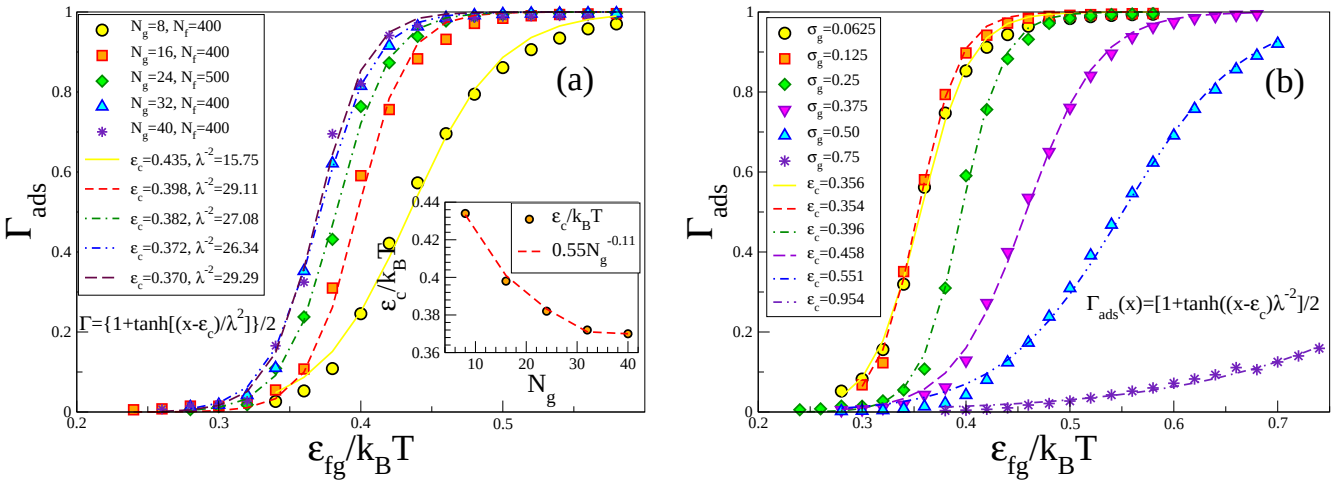

FIG. 2: (a) Adsorbed amount Γ_{ads} of a free chain with $N_f = 400$ segments in a polymer brush with $\sigma_g = 0.25$ as function of the brush - free chain attractive interaction ε_{fg}. The length of the chains N_g comprising the polymer brush is given as a parameter. In the inset, the critical strength of absorption, $\epsilon_c = \varepsilon_{fg}^c$, is shown to decrease with growing N_g and reach saturation for $N_g \geq 40$. (b) Γ_{ads} vs brush - free chain interactions ε_{fg} at fixed $N_g = 16$, $N_f = 400$, and different σ_g. Evidently, ϵ_c, and the transition interval λ^2 increase with growing σ_g which hampers the penetration of the free chain into the brush. The $\Gamma_{ads} - \varepsilon_{fg}$-relationship is interpolated here by an analytic function, $\Gamma_{ads} = \{1+\tanh[(\varepsilon_{fg}-\epsilon_c)/\lambda^2]\}/2$, which yields estimates for the critical adsorption strength, ϵ_c, and the width λ of the adsorption interval. Note that for $N_g = 16$ the brush-to-mushroom overlap grafting density is estimated to be roughly at $\sigma_g^* \approx 0.048$.

To characterize the absorption (or adsorption, respectively), we define the adsorbance $\Gamma_{\rm ads}$ as $\Gamma_{\rm ads} = N_{\rm ads}/N_f$, where $N_{\rm ads}$ is the number of monomers with z-coordinates $z < h$. Here the brush height h is defined, somewhat arbitrarily, by the condition that the density profile $\rho(z)$ of the brush monomers contains 99% of all the brush monomers when it is integrated from $z = 0$ to $z = h$. Remember that for N_g finite the profile $\rho(z)$ does not develop a sharp cutoff at $z = h$, but there is rather some "tail" of the density profile for $z > h$ that decays exponentially towards zero[36]. Figs. 2, 11 show the adsorbance defined in this way as a function of ε_{fg}, varying either N_g (Fig. 2a) or σ_g (Fig. 2b; see also Fig. 11 below). Empirically, $\Gamma_{\rm ads}$ can be fitted by a tanh function (note that a factor $1/k_BT$ is absorbed in the definition of ε_{fg}.)

$$\Gamma_{\rm ads} = \{1 + \tanh[(\varepsilon_{fg} - \varepsilon_{\rm fg}^{\rm c})/\lambda^2]\}/2 \quad . \tag{30}$$

From Fig. 2a one can recognize that for increasing N_g the critical value ε_{fg}^c shifts to smaller values, but this decrease stops and for $N_g = 32$ and $N_g = 40$ the curves almost superimpose. The energy interval over which the adsorption takes place narrows down somewhat when either N_g increases, or σ_g (Fig. 2b) decreases. It is remarkable that for $\sigma_g = 0.0625$ and $\sigma_g = 0.125$ the data almost superimpose (Fig. 2b) while for larger σ_g a larger energy ε_{fg} is needed to cause adsorption whereby the variation with ε_{fg} becomes more gradual. This trend is opposite to what one would expect on the basis of the theory of Section II C; but the explanation of this at first sight puzzling fact is that the simulation results address a parameter regime that is complementary to the regime for which the theory is supposed to hold. This fact will become more evident in the section on the SCFT treatment.

For a correct interpretation of the simulation results, it is useful to study the monomer density profiles of both the brush chains and the extra chain explicitly (Fig. 3). It is seen that for $N_g = 8$ the brush height is still less than 10 Lennard-Jones diameters only, and then it is hardly possible to bind all the monomers of a long adsorbed chain ($N_f = 400$) inside of the brush. For $N_g \geq 16$, however, and large ε_{fg}, the distribution function has its peak always deeply inside of the brush. One always finds that the free chain is bound to the brush surface near $\varepsilon_{fg} = \varepsilon_{fg}^c$. Since the distribution function of the strongly adsorbed chain (which has its maximum at about $z = 0.6h$) clearly broadens with increasing N_g (and hence increasing h), one sees that the general idea that the absorbed chain forms "blobs" of diameter comparable to brush height h seems to be confirmed by the simulation. Since the case $\sigma_g = 0.0625$ and $N_g = 16$ due to its relatively not so extremely large number of monomers (for linear dimensions $L_x = L_y = 40$ Lennard-Jones units we have $N_{ch} = 100$ chains and hence for $N_f = 400$ only four times more brush monomers, while for $\sigma_g = 0.25$, $N_g = 40$ (Fig. 2) the number of brush monomers is 16000 and hence forty time larger) is more favorable for a detailed study. Note that in the case $N_g = 40$ and ϵ_{fg}=0.34 the free chain is still spread out over almost the full

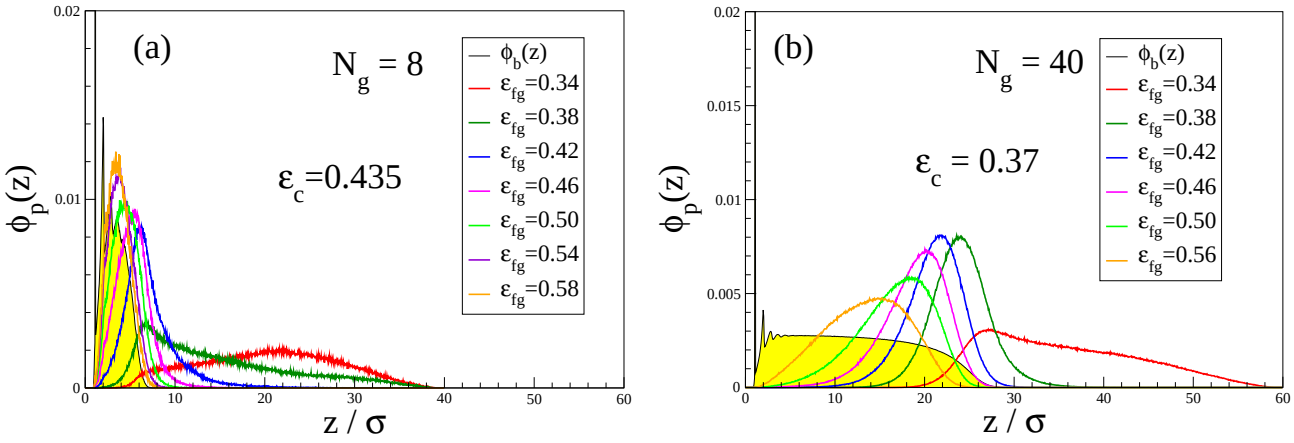

FIG. 3: Monomer density profile $\phi_b(z)$ of a polymer brush (yellow shaded) comprising $N_{ch} = 400$ chains of length $N_g = 8$ (panel a) and $N_g = 40$ (panel b) at grafting density $\sigma_g = 0.25$ and of a free chain, $\phi_p(z)$. Different strengths of interaction ϵ_{fg} between the brush- and free chain monomers are given as parameter. The free chain has length $N_f = 400$. Box size $40 \times 40 \times L_z$ with $40 \leq L_z \leq 60$.

volume outside of the brush, and hence these data are still slightly affected by the finite size of L_z. We also note that for the case of $N_g = 8$, $N_f = 400$, $\sigma_g = 0.25$, and ϵ_{fg}=0.435, a very slight swelling of the brush (on the order of 4%) is observed due to the adsorption of the free chain.

In the interpretation of such data one has to be very careful, however. This is demonstrated in Fig. 4: Plotting the adsorbed amount vs. ε_{fg} for $N_g = 8$, $\sigma_g = 0.25$ and four different chain lengths $N_f = 100, 200, 300$ and 400, at first sight one might conclude that the dependence of the data on N_f is negligible, and one has a gradual variation of $\Gamma_{\rm ads}$ with ε_{fg}, irrespective how large N_f is. If this conclusion were true, the results would be in strong contradiction with the physics of polymer adsorption, as exposed in Section II. In fact, from the results of Section II we can conclude that for $N_f \to \infty$ the result must be (taking $\phi = 1/2$ for simplicity)

$$\Gamma_{\rm ads}(\varepsilon_{fg} \leq \varepsilon^a_{fg}) = 0 \tag{31}$$

$$\Gamma_{\rm ads}\left(\varepsilon_{fg} > \varepsilon^a_{fg}\right) \propto \left(\frac{\varepsilon_{fg}}{\varepsilon^a_{fg}} - 1\right) = t \quad , \tag{32}$$

where $\varepsilon_{fg}/\varepsilon^a_{fg}$ was denoted as T_a/T in Section II: so $T_a \propto 1/\varepsilon^a_{fg}$ is the actual transition temperature of the adsorption transition. By fitting a straight line to the data in the regime $0.1 < \Gamma_{\rm ads} < 0.4$, one would conclude that $\varepsilon^a_{fg} \approx 0.37$, rather different from the value of the inflection point ($\varepsilon^c_{fg} \approx 0.435$).

Another criterion could be based on the adsorption energy: if the extra chain is not adsorbed, the internal energy U_{fg} of the system actually should be independent of ε_{fg} since no contacts between monomers of the brush and of the extra chain occur. In the regime where the chain is absorbed, however, we expect that U_{fg} should be proportional to ε_{fg}. Thus, we expect that the derivative of U_{fg} with respect to ε_{fg} should jump from zero for $\varepsilon < \varepsilon^a_{fg}$ to a nonzero value for $\varepsilon > \varepsilon^a_{fg}$. This is tested with the result, that the transition should be in the region $0.30 < \varepsilon^a_{fg} < 0.36$ (of course, for finite N_f the sharp transition is rounded off over some interval). In practice, one does find that the derivative U'_{fg} is zero for the clearly non-adsorbed chains, then it rises to a rather well-defined maximum, and thereafter decreases again, Fig. 4b.

It is instructive to consider what the theory of the adsorption transition (Section II A) implies regarding the inflection point of the adsorbance studied as function of ε_{fg}. One may assume that the adsorbance can be taken to represent the ratio N_s/N_f, which near the adsorption transition behaves as $N_s/N_f = N_f^{\phi-1}\tilde{N}(\zeta)$ where $\zeta = tN_f^{\phi}$, see Eq. (5).

Now, a basic point of the theory is that for N_f finite, the scaling function $\tilde{N}(\zeta)$ is an analytic function of its argument ζ; i.e., we can write down a power series expansion

$$\tilde{N}(\zeta) = a + b\zeta + c\zeta^2 + d\zeta^3 + \cdots .... \quad . \tag{33}$$

Here $a > 0$, $b > 0$, $c > 0$ must be positive constants since N_s is nonzero for $\varepsilon_{fg} = \varepsilon^a_{fg}$ and has a positive slope and positive curvature ($\tilde{T}(\zeta)$ is concave at $\zeta = 0$). In order to have an inflection point at $\zeta > 0$, we assume $d < 0$ (if we would have $d > 0$, the same conclusion follows taking coefficients of higher order terms negative). We now find the location of the inflection point, where the function $\tilde{N}(\zeta)$ changes from concave to convex, from

$$\frac{d^2\tilde{N}(\zeta)}{d\varepsilon^2_{fg}} = \frac{d^2\tilde{N}(\zeta)}{d\zeta^2}\left(\frac{d\zeta}{d\varepsilon_{fg}}\right)^2 = 0 \tag{34}$$

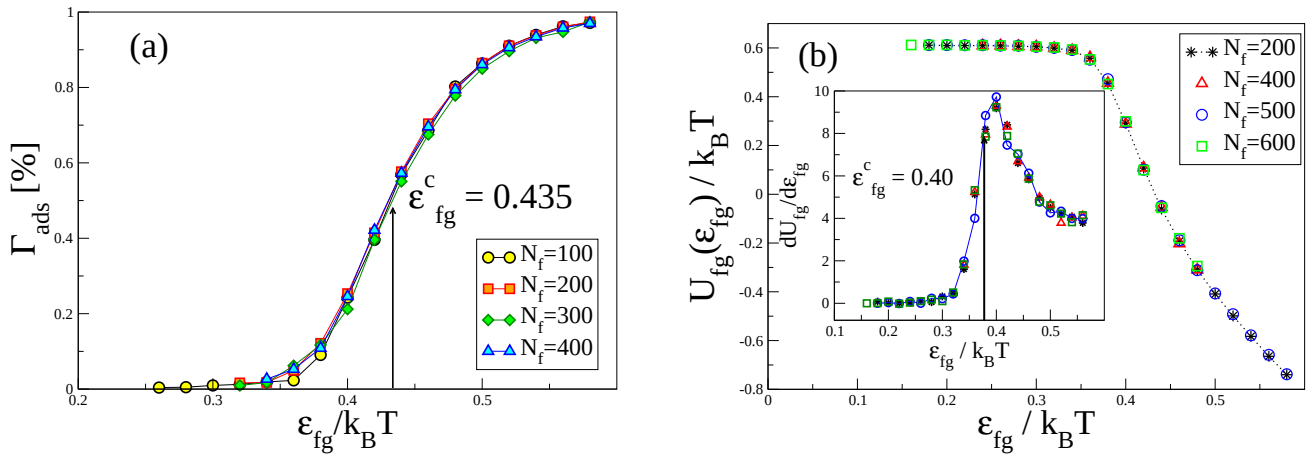

FIG. 4: (a) Adsorbed amount Γ_{ads} vs interaction strength ϵ_{fg} for a polymer brush with $N_g = 8$, $\sigma_g = 0.25$ and different length of the free chain N_f, given as a parameter. Here interpolation by means of a tanh-function yields $\epsilon^c_{fg} \approx 0.435$. Evidently, Γ_{ads} is largely insensitive with regard to N_f. (b) Internal energy U_{fg} vs interaction strength ϵ_{fg} between polymer coating and adsorbing chains for chains of different length N_f (given as parameter) and grafting density $\sigma_g = 0.25$. The first derivative U'_{fg} goes through a maximum at ϵ^c_{fg}: here $N_g = 16$.

as

$$\zeta_{\rm infl} = \frac{c}{3|d|}, \quad \frac{\varepsilon^{\rm infl}_{fg}}{\varepsilon^a_{fg}} - 1 = N_f^{-\phi}\frac{c}{3|d|} \quad . \tag{35}$$

Thus, the location of the inflection point $\varepsilon^{\rm infl}_{fg}$ indeed moves towards the location of the adsorption transition (ε^a_{fg}) as $N_f \to \infty$. However, the value of $\tilde{N}(\zeta = \zeta_{\rm infl})$ is also a constant of order unity, and hence N_s/N_f at $\varepsilon^{\rm infl}_{fg}$ is proportional to $N_f^{\phi-1} \to 0$ as $N_f \to \infty$. Hence, an inflection point at $N_s/N_f = 1/2$ independent of N_f (as implied by the fit of Eq. (30) with the tanh function) clearly disagrees with the theory of the adsorption transition (Section II.1).

The behavior seen in Fig. 4b is not compatible with expectations, one finds instead that the derivative of the internal energy shows a maximum near ε^c_{fg}. This maximum gets sharper with increasing chain length N_g of the grafted chains while the dependence on N_f seems to be negligibly small. This behavior clearly is not yet understood.

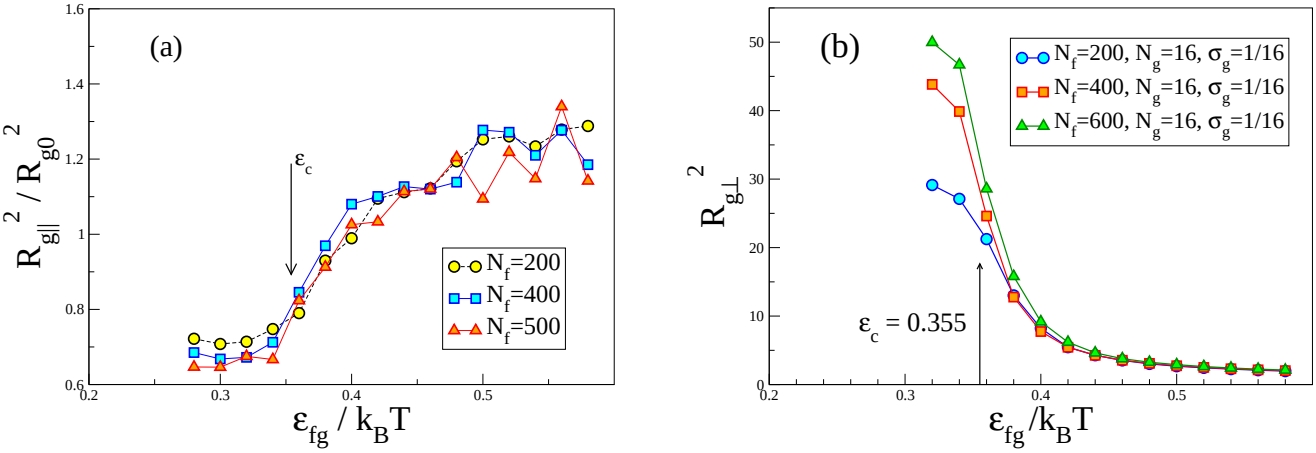

FIG. 5: Gyration radius components of the free chain, $R^2_{g||}$, $R^2_{g\perp}$ vs interaction strength ϵ_{fg} between polymer brush and adsorbing chains of length N_f (given as parameter). Here $N_{ch} = 400$, $N_g = 16$ and $\sigma_g = 0.0625$.

Now, in the case of the simple lattice models [20] the most frequently used criterion to locate the adsorption transition is based on the gyration radii components parallel ($R^2_{g||}$) and perpendicular ($R^2_{g\perp}$) to the adsorbing substrate. We have tried this for our model for the case $\sigma_g = 0.0625$ and $N_g = 16$ (Fig. 5). As expected, $R^2_{g\perp}$ becomes independent of N_f for $\varepsilon_{fg} \gg \varepsilon^a_{fg}$ (then $R^2_{g\perp}$ is a measure of the mean square thickness of the "pancake", of course). In the transition region, one can see the expected finite chain length effects, but the statistical errors are still too large to allow a quantitatively reliable analysis in terms of Eq. (6). For the parallel component (Fig. 5a) the situation, unfortunately, is worse: while the location of the inflection point of the curves is roughly compatible with the estimate $\varepsilon^c_{fg} \approx 0.355$

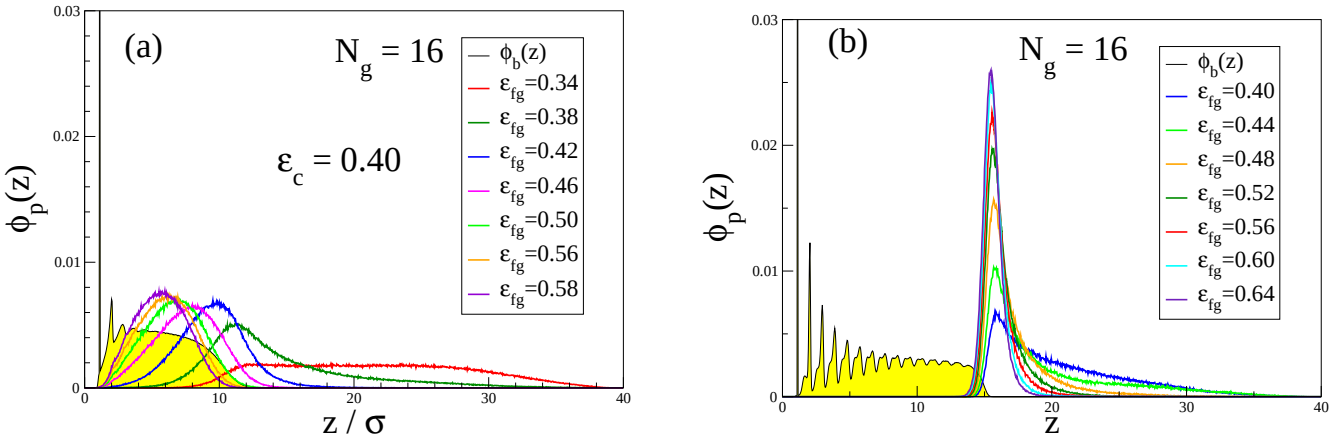

FIG. 6: (a) Monomer density profile $\phi_b(z)$ of a polymer brush (yellow shaded) comprising $N_{ch} = 400$ chains of length $N_g = 16$ at grafting density $\sigma_g = 0.25$ and of a free chain, $\phi_p(z)$. Different strengths of interaction ϵ_{fg} between the brush- and free chain monomers are given as parameter. The free chain has length $N_f = 400$. (b) The same at grafting density $\sigma_g = 0.75$.

extracted from the adsorbance inflection point, the statistical averaging of the data points remains rather poor even after 10^{10} integration steps (i.e., taking a single processor computational effort of 6 months)! A check of the mean square displacement of the center of mass, r_{CM}, of an absorbed $N_f = 400$-bead chain has revealed that after 5×10^6 integration steps (i.e., $\approx$ 55 hours CPU), r_{CM} has moved only about 2σ away from its initial position. Therefore, apparently when a long chain is absorbed in the brush, its configuration can equilibrate only locally whereas the large scale configuration in direction parallel to the surface remains out of equilibrium during the time scales accessible to MD. Thus, while in principle Molecular Dynamics simulations are a method that should be superior to the theory presented in Section II, where numerous crude approximations needed to be made, in practice the advantage of MD is offset by the difficulty to obtain statistically significant data. It would be interesting to try to study this problem by Monte Carlo simulations applying an optimized set of moves (slithering snake moves, configurational bias cut-and-regrowth moves, etc.) but such an approach clearly is a major project of its own right and is out of scope of the present work.

Finally, Fig. 6 shows profiles of the monomer density of the polymers in the brush and of the absorbed chain for the case of a very high grafting density, $\sigma_g = 0.75$ (and $N_g = 16$, $N_f = 400$). There occurs a strong layering of the density near the wall and the chains are strongly stretched in the brush (remember that the typical distance between subsequent monomers along a chain is 0.96, and hence with $h \approx 15$ the brush chains are stretched almost rod-like). In this case the monomers of the free chains cannot penetrate in the brush, and are rather adsorbed at the brush-solution interface, as if this interface would be a planar wall. From the change of the profiles of the monomers density of the free chain with ε_{fg} we see that for $\varepsilon_{fg} \approx 0.40$ to 0.48 the tail of the profile reaching far out into the region $z \gg h$ is strongly diminishing. So $\varepsilon^a_{fg} \approx 0.44$ is a preliminary estimate for the location of the adsorption transition.

V. TREATMENT BY SELF-CONSISTENT FIELD THEORY AND DENSITY FUNCTIONAL THEORY

The technique which we use here is the Scheutjens-Fleer [2, 45, 50, 51] lattice formulation of the self-consistent field theory (SCFT) of polymeric systems. This method is well-known and has been described many times; it goes beyond Flory-type approximations since it can describe spatially inhomogeneous distributions of the monomers, although like the Flory approximation (see [45] for a recent discussion) it has some problems in predicting the correct scaling of the free energy of chains in the dilute limit, and it cannot describe critical exponents of the adsorption transition beyond the Flory mean field level. But it has the distinct advantage that unlike simulation approaches it is not plagued by statistical errors, and with relatively little computational effort (particularly in cases when only one-dimensional inhomogeneities $\rho(z)$ of the monomer density ρ in the z-direction perpendicular to the grafting surface $z = 0$ need to be considered) very long chains can be studied. For technical details of our formulation, we refer to our previous papers [45, 46], and only note that we use a simple cubic lattice, using the lattice spacing as unit of length in the present section, which is also the distance between adjacent monomers along a chain. In our model, grafting densities σ_g from zero to unity can be studied.

When one wishes to compare the SCFT results to the MD results, however, one must be aware that there is no straightforward correspondence between the parameters of both models: the length unit of SCFT (lattice spacing) does not strictly correspond to the range σ of the repulsive potential of the off-lattice model, and so the grafting densities σ_g in the present section cannot be directly identified with those of the MD section. Likewise, it is not clear whether the chain lengths on the lattice can be directly identified with those in the continuum model. In principle, one would need to find suitably scaled dimensionless variables that could be compared. A similar difficulty concerns the precise conversion of the Lennard-Jones parameter ϵ_{fg} to the Flory-Huggins parameter χ_{FH}. At the present stage of our study, an attempt at a quantitative conversion of parameters between both approaches was judged to be a too

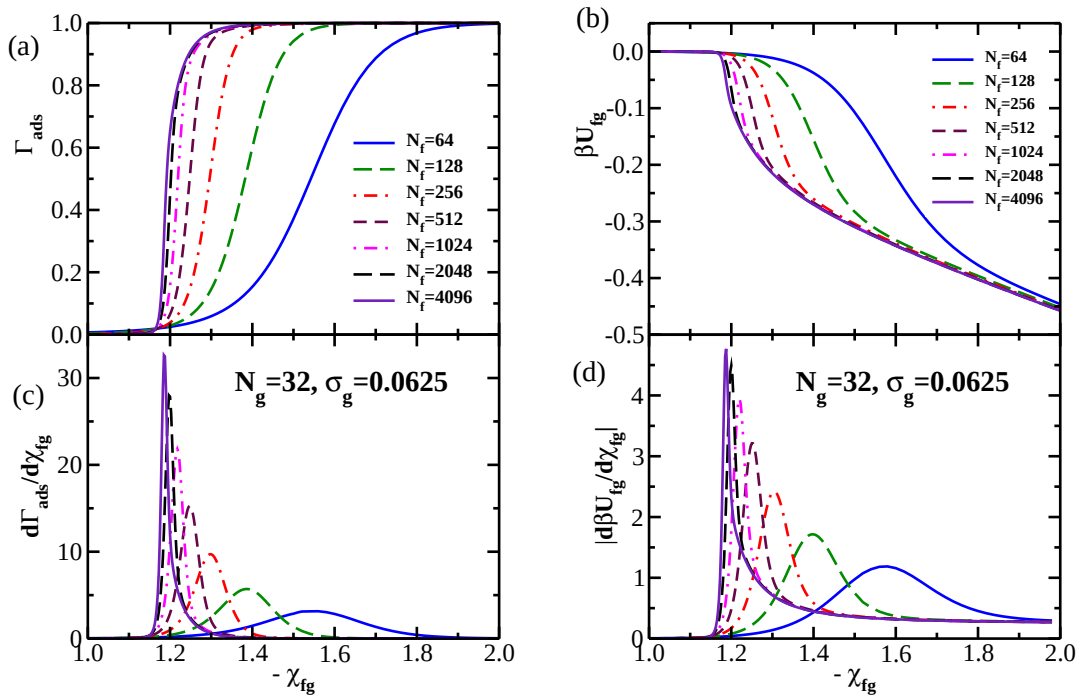

FIG. 7: SCFT results for the variation of the relative adsorbed amount Γ_{ads}, (a), and of the total interaction energy U_{fg} between the monomers of the free chain and the grafted chains (b), plotted versus the Flory-Huggins parameter $|\chi_{fg}|$, for the case $\sigma_g = 0.0625$, $N_g = 32$, and several choices of the chain length N_f of the free chains, namely $N_f = 64, 128, 256, 512, 1024, 2048,$ and 4096. Parts (c) and (d) show the derivatives $d\Gamma_g/d|\chi_{fg}|$ and $dU_{fg}/d|\chi_{fg}|$ as functions of $|\chi_{fg}|$, for the same choices as a) and b), respectively.

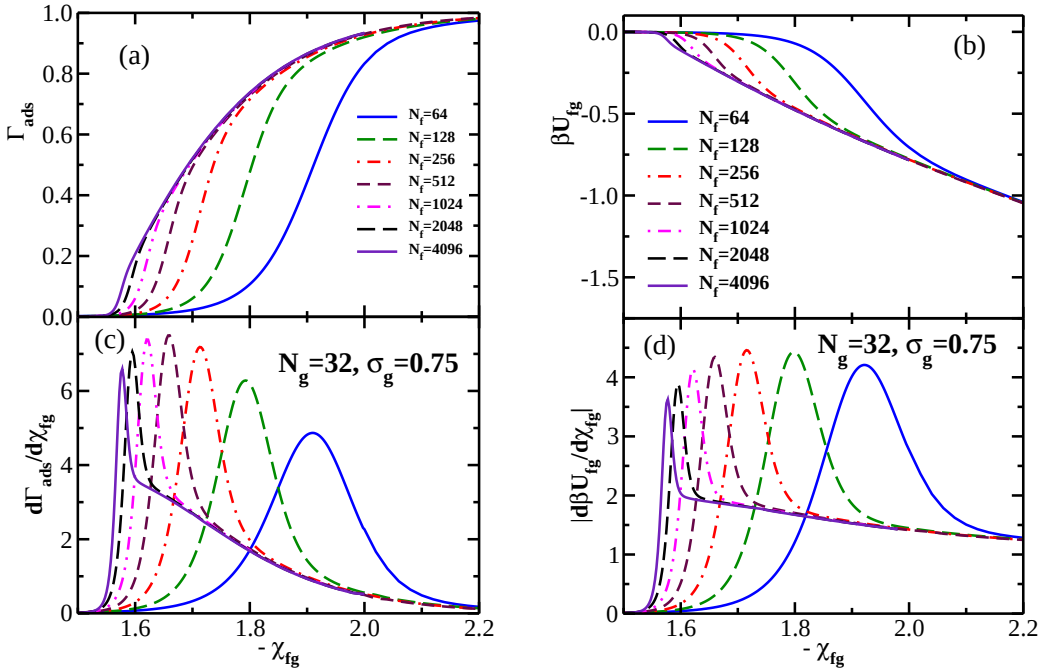

FIG. 8: Same as Fig. 7, but for $\sigma_g = 0.75$

ambitious task, particularly in view of the fact that certain features (like the finite-size effects regarding N_f) differ even qualitatively.

Figs. 7-8 present typical data. Unlike the simulation (Figs. 4, 5), where for the corresponding data the dependence of the results on the chain length N_f could not be disentangled from the statistical errors (of course, only a much smaller range of variation, by a factor of 4 rather than 64, was accessible via MD), now the systematic dependence on N_f is clearly displayed, and an analysis of the SCFT data along the lines of the theory could be attempted. We emphasize, however, that the combinations of parameters that are similar to those used in the MD work, e.g., $N_f = 128 \div 512$, $\sigma_g = 0.0625$ (Fig. 7), the general shape of the adsorbance as function of inverse temperature

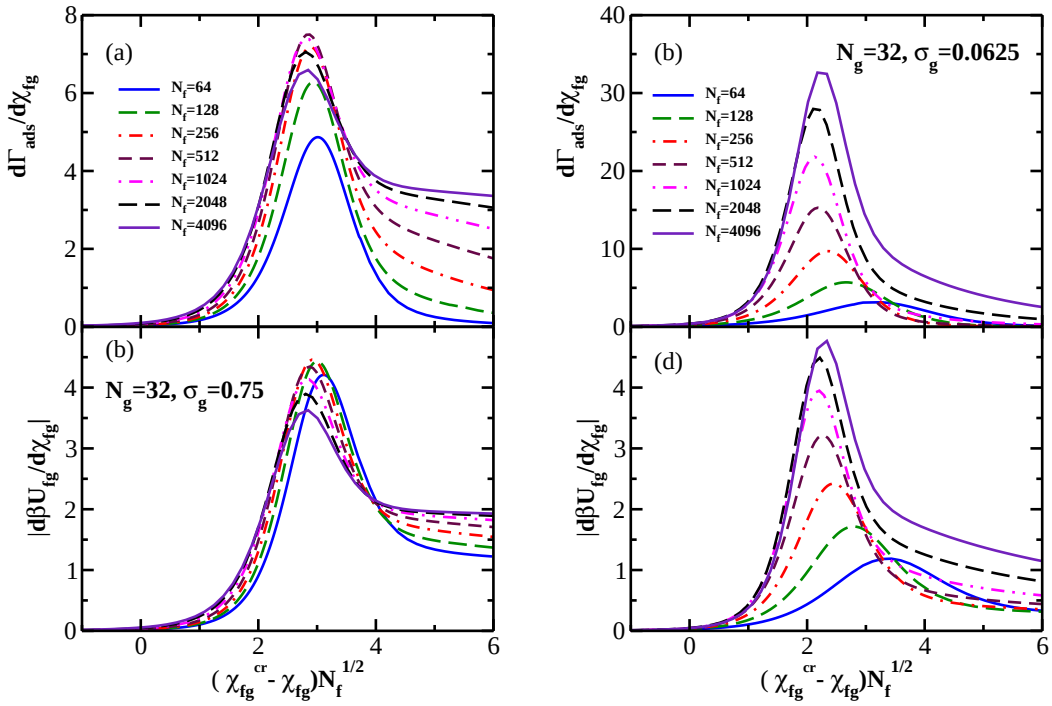

FIG. 9: Upper panels: SCFT results for the derivative $d\Gamma_{ads}/d|\chi_{fg}|$ plotted as a function of the scaling variable $(\chi_{fg}^{cr}-\chi_{fg})N_f^{1/2}$ for two values of the grafting density: $\sigma_g = 0.75$ (a), and $\sigma_g = 0.0625$ (b). The results are given for the grafted chain length $N_g = 32$ and for several choices of the chain length N_f of the free chains, namely $N_f = 64, 128, 256, 512, 1024, 2048$, and 4096. Lower panels: same as above, but for the derivative $dU_{fg}/d|\chi_{fg}|$.

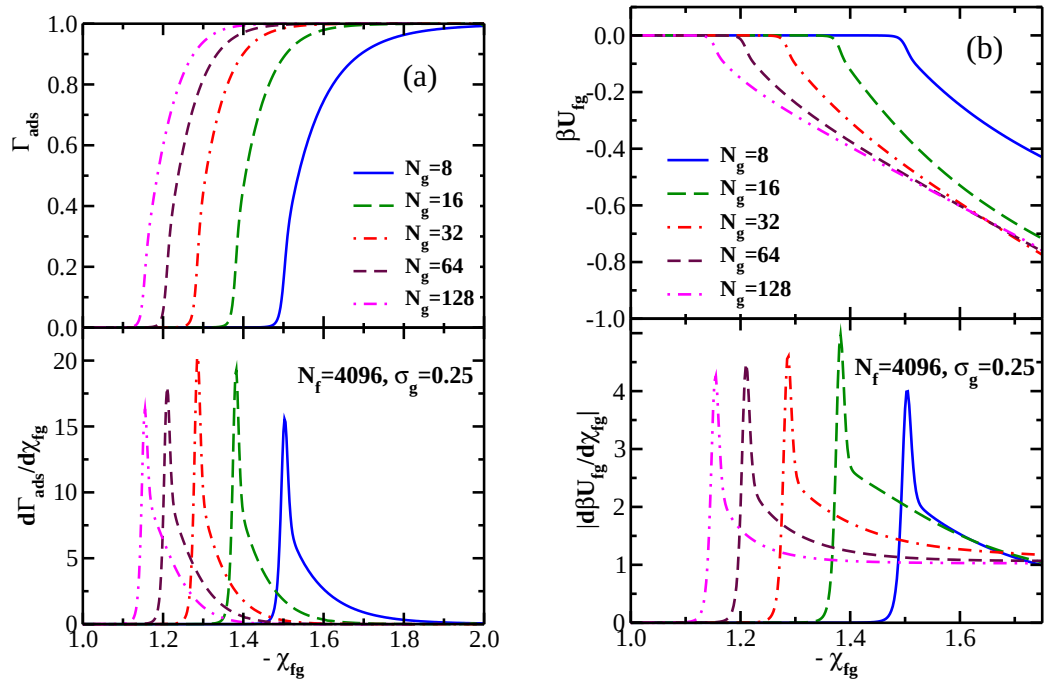

FIG. 10: (a) Plots of adsorbance Γ_{ads} (upper part) and its derivative $d\Gamma_{ads}/\chi_{fg}$ (lower part) vs Flory-Huggins parameter $-\chi_{fg}$ for the case $N = 4096$, $\sigma_g = 0.25$, varying N_g from $N_g = 8$ to $N_g = 128$, as indicated. (b) Adsorption energy βU_{fg} (upper part) and its derivative, $d\beta U_{fg}/d\chi_{fg}$ (lower part) for the same cases as shown in part (a).

(Fig. 2), and also the desorption energy and its derivative, (Fig. 7b), are qualitatively very similar to their simulation counterparts (such as the example included in Fig. 4b. Data for other parameter choices look very similar and were not shown to save space). The only qualitative difference is that in the simulation, data for $N_f = 100$ to 400, or 200 to 600 always coincide within error. We attribute this fact to the hypothesis that only subchains of length $n < N_f$ attain local equilibrium when they are absorbed in the brush while the global parallel linear dimensions of the chain are still "frozen" on the time scale accessible to MD, and hence entropic effects due to the variation of the properties with N_f are not seen. This freezing of parallel linear dimensions is due to entanglement of the chain with the densely-grafted

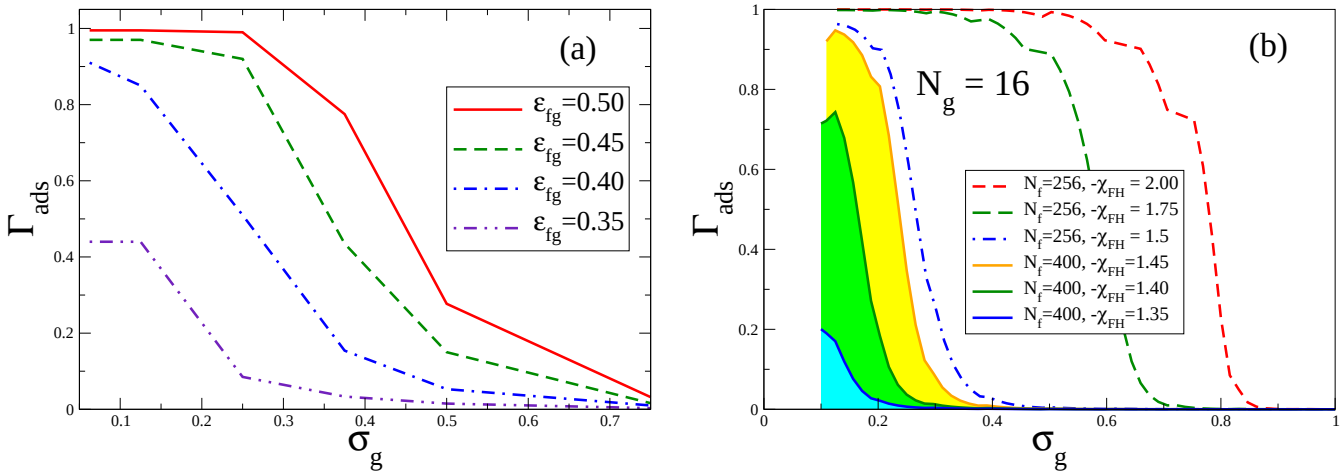

FIG. 11: (a) MD data for the variation of adsorbance Γ_{ads} with σ_g for a free chain with $N_f = 400$ segments in a polymer brush with $N_g = 16$ and different ε_{fg}, given as parameter. (b) The same for changing parameter χ_{FH} from SCFT calculations: full curves (shaded) are for $N_f = 400$, dashed lines correspond to $N_f = 256$. Note that in the MD work only a few values of σ_g were studied, and then the results for $\Gamma_{ads}(\sigma_g)$ were connected by straight lines, to guide the eye.

brush chain which act like linear frozen obstacles, extended from $z = 0$ to $z = h$, on the chain motion and this topological interaction between brush chains and the free chain is responsible for the metastability observed in the MD simulation.

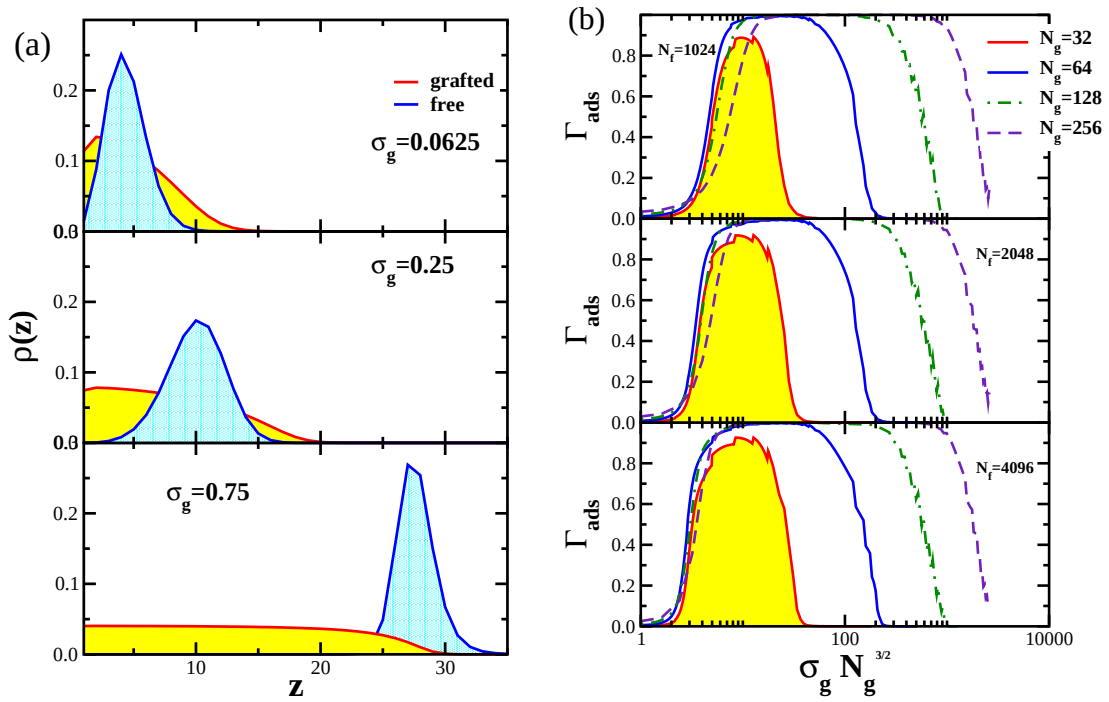

FIG. 12: (a) Density profiles of the polymer brush (yellow-shaded) and of the free chain (shaded in blue) for the case $N_g = 32, N_f = 4096, \chi_{fg} = -1.8$ and three choices of grafting density $\sigma_g = 0.0625,\ 0.25,\ 0.75$, as indicated. A gradual transition from free chain absorption to expulsion is observed with growing σ_g. (b) Adsorbance Γ_{ads}, plotted vs $\sigma_g N^{3/2}$. Three choices for N_f are shown for $\chi_{fg} = -1.25$ and $N_f = 1024$ (upper plot), $N_f = 2048$ (middle plot), and $N_f = 4096$ (lower plot), and four choices of N_g, as indicated.

From Figs. 7-8 several general conclusions emerge: (i) for finite N_f the peak positions of the adsorbance- and the adsorption energy derivatives are always shifted to significantly larger values of $-\chi_{fg}^{max}$, the difference $|\chi_{fg}^{max} - \chi_{fg}^{c}| \propto 1/\sqrt{N_f}$ in all cases. (ii) While for small σ_g the peak heights of these maxima increase strongly with N_f, for large σ_g there is only a weak increment for relatively small N_f, then a finite maximum peak height is reached. We also note that the variation of Γ_{ads} and U_{fg} with $-\chi_{fg}$ is very steep for small σ_g, Fig. 7, and very moderate for large σ_g, Fig. 8.

Eq. (7) suggests re-writing the derivative of the relative adsorbance with respect to χ_{fg} in the following scaling

form:

$$\frac{d}{dt}\frac{N_s}{N_f} = N_f^{2\phi-1}\ \tilde{N}_f'\{tN_f^{\phi}\} = \tilde{N}_f'\{tN_f^{1/2}\} \quad , \tag{36}$$

where we have set $\phi = 1/2$, and $t = 1 - \chi_{fg}/\chi_{fg}^{cr}$. Our SCFT results for the derivative of Γ_{ads} with respect to χ_{fg} are re-plotted in the upper panels of Fig. 9 according to the scaling relation given by Eq. (36) for two values of the grafting density: $\sigma_g = 0.75$ (panel a) and $\sigma_g = 0.0625$ (panel b). Note that according to the scaling result, the peak height of the derivative should be independent of the free chain length N_f. While this prediction holds reasonably well in the case of higher grafting density (at least for $N_f > 1000$), it does not hold for $\sigma_g = 0.0625$ (where one would need to go at least beyond $N_f = 4096$ to observe scaling). This is to be expected, as in the case of the high grafting density the free chain is located primarily in the outer region of the brush, while at the low grafting density it penetrates the entire brush, which (due to the blob effects mentioned in Section IIB) means that the chains, used in deriving the scaling result above, are effectively much shorter. These SCF results also demonstrate that it would be impractical to attempt to observe scaling behavior via either MD or MC simulations, as it would require using extremely long free chains.

A special advantage of SCFT is that a broad variation of parameters is feasible with a manageable computational effort. Thus, we have also studied the effect of varying N_g over a wide range - Fig. 10. As expected, the critical value of the Flory-Huggins parameter where adsorption occurs shifts to smaller values as N_g increases, since the chain penetrates it. Also, in contrast to the behavior observed in Figs. 7-8, varying N_g while keeping all other parameters constant seems to just shift similar curves without changing their shape, Fig. 10.

One should not claim too hastily that the SCFT simulations are fully in qualitative accord with the theory of Section II, Eq. (24) implies that the critical value of ϵ_{fg} decreases with increasing grafting density σ_g. Consequently, at fixed ϵ_{fg} one should expect that the adsorbance *increases* with increasing σ_g. However, both MD and SCFT agree (see Fig. 11) with respect to the finding, that in the range from $0.15 \leq \sigma_g \leq 0.8$ the opposite behavior happens, namely the adsorbance *decreases* with growing σ_g, irrespective of the choice of ϵ_{fg} (MD simulation), or χ_{FH} (SCFT), respectively!

One should not be worried, of course, that results for the same values of parameters ($N_g = 16,\ N_f = 400$) for MD and SCFT are not in quantitative agreement, cf. Fig. 11, as has already been stressed above, there is no one-to-one correspondence between σ_g (MD) and σ_g (SCFT), nor between N_f (MD) and N_f (SCFT), etc. Indeed, a small change of N_f ($N_f = 256$ instead of $N_f = 400$) brings the SCFT results into the same region of σ_g as the MD data! Clearly, any attempt at a quantitative comparison between MD and SCFT at this stage would be premature.

However, from the *qualitative* discrepancy between Fig. 11 and the theory of Section II one must not conclude that this theory is useless; the correct interpretation is rather that the theory for the shown grafting densities is not applicable, and one should work at much smaller grafting densities σ_g (and, correspondingly, larger N_g) so that the mean-field type approximations underlying the theory work better. This aspect of the problem will be studied next.

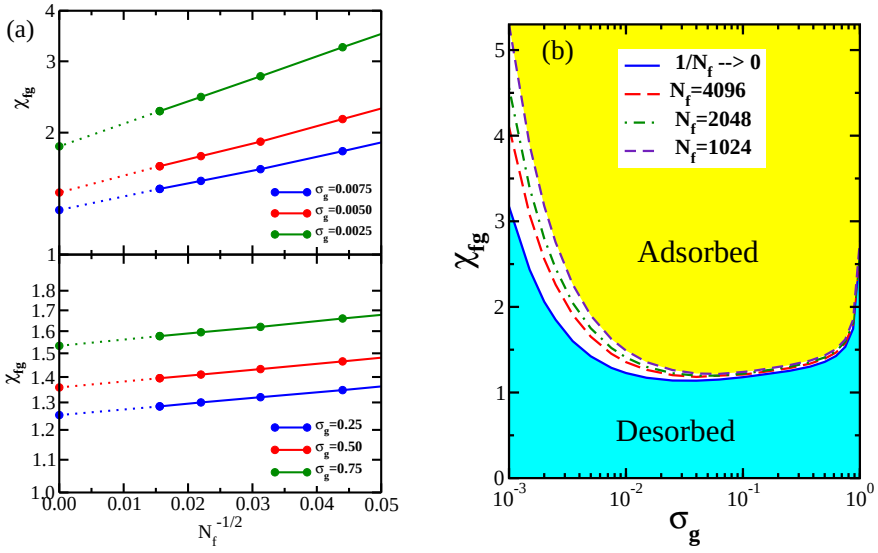

FIG. 13: Estimated location of the adsorption phase transition from plotting the locations of the maxima of $|d\Gamma_{ads}/d\chi_{fg}|$ vs $N_f^{-1/2}$ for 6 different values of σ_g, as indicated. All data are for $N_g = 32$. (b) Final "phase diagram", according to the SCFT prediction for the case $N_h = 32$, in the plane of variables χ_{fg} (ordinate) and σ_g (abscissa; note the logarithmic scale). Broken lines denote the locations of the (rounded) transitions for finite N_f, full curve the result of the extrapolation. The free chain is bound to the brush (either absorbed inside the brush at small σ_g, or adsorbed on the brush surface for larger σ_g), if χ_{fg} is above the shown curve(s).

An interesting question concerns also the validity of predictions such as Eq. (24) which states that in the semidilute regime ($\sigma_g \to 0,\ N_g \to \infty$) the critical value for the Flory-Huggins parameter should not depend on $\sigma_g N_g$ separately, but rather on the combined variable $\sigma_g N_g^{3/2}$ only. Thus, when we vary these parameters individually, but keep their

product unchanged, the adsorbance Γ_{ads} should simply be a function of this product only. This is tested in Fig. 12b in the limit of very small σ_g for $N_f = 4096$, and is found to be satisfied reasonably well. It must be emphasized, however, that this scaling fails completely for large grafting densities, Fig. 12b, and one finds that actually then the adsorbance decreases again. The reason for this breakdown of the scaling, incorporated in the theory of Section II, is that for large grafting densities the chains are no longer *absorbed* into the brush but are at least *adsorbed* at the outer surface of the brush, or even expelled completely from it. This is seen very directly when one looks at the density profiles of the chains in relation to those of the grafted ones - Fig. 12a. Note that in this SCFT formulation one can choose the monomer concentration of the very dilute solution at a large distance L_z from the brush (or the associated osmotic pressure) as a input parameter, and compute the adsorbance as the monomer excess density that is found inside the brush. In this way a spurious L_z-dependence is avoided.

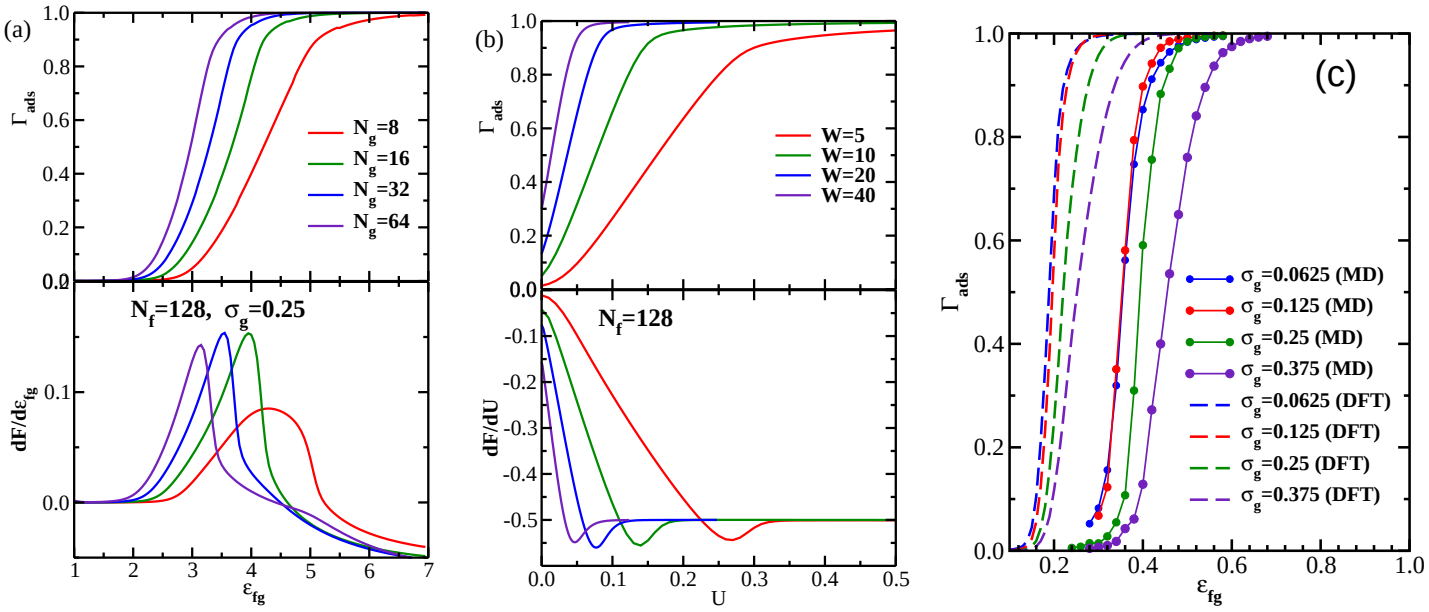

FIG. 14: Direct comparison of the adsorbance Γ_{ads} and the derivative of the free energy with respect to the interaction strength for a single chain adsorption in a brush vs square-well potential. The free chain length is $N_f = 128$. (a) Polymer brush with grafting density $\sigma_g = 0.25$ and four different lengths of the grafted chains $N_g = 8, 16, 32, 64$. (b) A square-well attractive potential with width $W = 5, 10, 20, 40$, roughly corresponding to the height of the brush. Apparently, the critical adsorption strength depends much weaker on brush height than on W. (c) Comparison of the Γ_{ads} vs ϵ_{fg} relationship for $N_g = 16$, $N_f = 400$ from MD and DFT computations.

Of course, for a quantitative discussion of this phenomenon again an extrapolation towards $N_f \to \infty$ is needed - Fig. 13. It is seen that in the $\chi_{fg} - \sigma_g$ plane the transition line for the adsorption (absorption) transition first decreases with σ_g, then reaches a shallow minimum, and for large σ_g increases again.

We summarize our finding obtained by SCFT as follows: (i) for all choices of σ_g and N_g that were studied, we have found that in the limit of long chains ($N_f \to \infty$) that are absorbed into the brush (or adsorbed on the brush / solvent interface, respectively) the transition follows the general theoretical framework of the polymer adsorption transition , as outlined in Section II. In particular, the rounding of the transition due to the finiteness of N_f is compatible with the theoretical expectation, Eqs. (33)-(35). Fig. 13a shows, as an example, that the transition in the limit $N_f \to \infty$ is always compatible with the expected scaling with $N_f^{-1/2}$. (ii) For typical cases of σ_g and N_g absorption (or adsorption, respectively) can occur only if the interaction strength $|\chi_{fg}|$ between the monomers of the free and the grafted chains is fairly strong. So, for instance, for $N_g = 32$ the minimum value of $|\chi_{fg}^{cr}|$ is larger than unity (and occurs in the semidilute limit $10^{-2} \le \sigma_g \le 10^{-1}$. For smaller σ_g, $|\chi_{fg}^{cr}|$ rises strongly, since one leaves the brush regime and crosses over into the mushroom regime. For dense brushes, $\sigma_g > 0.5$, one observes an increase of $|\chi_{fg}^{cr}|$ again, because the chain can no longer be absorbed into the brush which would require then too much elastic energy of the brush chains, therefore, one can only find adsorption on the brush-solution interface. The change in character of the absorption phenomenon is also evident from the fact that for absorption at small σ_g, Fig. 7, the adsorbance reaches saturation already for $|\chi_{fg}| \approx 1.2|\chi_{fg}^{cr}|$ while for large σ_g, Fig. 8, saturation is only reached for $|\chi_{fg}| \approx 1.5|\chi_{fg}^{cr}|$.

In order to elucidate further the physical distinction between adsorption of a chain in a square well potential of width W and in a brush of height $h \propto W$, we have carried out a comparative study of both cases via Density Functional calculation (DFT), Fig. 14. For details about this method in the context of polymer brushes, we refer to [52, 53]. In both cases we varied W (or, h) by a factor of 8. While for the square well potential indeed the critical value $U_c(W) \to 0$ with $W \to \infty$, in the polymer brush this is not the case when N_g increases, Fig. 14.

As shown in Fig. 14c, the variation of the adsorbance with ϵ_{fg} and grafting density as predicted by DFT is quite similar to the corresponding MD results, apart from a mismatch of the energy scale.

It is seen that the DFT results for brushes (Fig. 14a,c) are qualitatively similar to the MD results (Fig. 2) and

to SCFT results (Fig. 10) while the behavior of the adsorbance Γ_{ads} vs U in the case of square-well potential is very different. So this method confirms the conclusions of the previous sections that a straightforward correspondence between adsorption of free chains by polymer brushes of height h and adsorption by square well potential of width W should not be expected.

VI. CONCLUDING REMARKS

In this paper we have studied the adsorption of single long flexible macromolecules in polymer brushes, considering good solvent conditions throughout, but allowing for an effective short-range attractive interactions between the brush monomers and the monomers of the free chain. We use both Molecular Dynamics simulations and numerical self-consistent field calculations to study various aspects of this problem, and discuss our results within the general theoretical framework that was developed for the polymer adsorption transition. Parameters that need to be varied are the properties of the brushes (their grafting density σ_g, chain length N_g) and the length of the free chain(N_f) as well as the strength ϵ_{fg} of the attractive interaction.

For typical combinations of parameters the transition by which the polymer is absorbed in the brush is rounded over a wide range of ϵ_{fg}, but this range gets somewhat narrower when either N_g increases (Fig. 2) or σ_g decreases (from $\sigma_g = 0.5$ to $\sigma_g = 0.0625$). However, for very small σ_g (e.g. $\sigma_g < 10^{-2}$, this regime was not accessible by MD but was easily accessed by SCFT) one needs very large ϵ_{fg} to still achieve absorption, of course. As a result, in the $\epsilon_{fg} - \sigma_g$ plane the phase boundary separating the desorbed regime from the adsorbed regime is reentrant (Fig. 13b). As a consequence, at fixed ϵ_{fg} (or, fixed Flory-Huggins parameter χ_{fg}) the adsorbance varies monotonically with σ_g: for small σ_g the free chains are absorbed into the brush when σ_g increases whereas for large σ_g the free chains are expelled again (Fig. 12b). These SCFT results are compatible with the MD findings (Fig. 11b) too. The absorption transition at small σ_g leads to a state where the density profiles of the free chain and the brush chains overlap strongly while near the transition at large σ_g the free chains are localized at the brush-solvent interface (Figs. 3,12b).

While the SCFT results fit qualitatively to the general theoretical framework (Section II) that has been developed for the adsorption transition, in particular, when N_f increases the transition becomes sharper (Figs 7, 8), and the positions of the peaks of derivatives which can be labeled as "effective" transition points show a shift (Fig. 13a) that is compatible with the theory, within MD the variation of N_f by factor of 3 or 4 (Fig. 4) does not seem to have any effect. Strong fluctuations of the parallel components of the gyration radius indicate (Fig. 5a) possible equilibration problems. This calls for a study of the dynamics of absorbed chains in brushes, however, such a study is beyond the scope of the present work.

We have also payed attention (Section II) to the mapping that has been proposed for the absorption of polymers in brushes, suggesting that there is an equivalence of a brush to square-well potential of the same width as the height of the brush. However, although this idea is clearly very appealing, it does not help much to interpret either the SCFT calculations, or the data from MD simulations. While the SCFT results clearly support that for long enough chains absorbed in polymer brushes the scaling description of the adsorption transition works, one needs much longer chains to reach this universal scaling regime, than when one considers adsorption in a simple square well potential. For the much shorter chains that are feasible to use in MD simulations, this scaling regime hence is not of practical relevance. Finally, we draw attention that our study may give a more detailed insight into the mechanism of polymer chromatography under critical conditions.

Acknowledgments

We are grateful to the Deutsche Forschungs Gemeinschaft (DFG), grant No. *BI* 314/23, and to the Schwerpunkt für Rechnergestützte Forschung in den Naturwissenschaften (SRFN) for partial support of this work, and thank L. I. Klushin and A. M. Skvortsov for stimulating discussions. S.A.E. acknowledges financial support from PRF Grant # 53934-ND6.

[1] E. Eisenriegler, *Polymers Near Surfaces*, (World Scientific, Singapore, 1993)
[2] G. J. Fleer, M. A. Cohen-Stuart, J. M. H. M. Scheutjens, T. Cosgrove, and B. Vincent, *Polymers at Interfaces* (Chapman and Hall, London, 1993)
[3] R. Simha, H. L. Frisch, and F. R. Eirich, J. Chem. Phys. **57**, 584 (1953)
[4] R.-J. Rubin, J. Chem. Phys. **43**, 2393 (1965)
[5] P. G. de Gennes, J. Phys. (France) **37**, 1445 (1976)
[6] T. M. Birshtein, E. B. Zhulina, and A. M. Skvortsov, Biopolymers **18**, 1171 (1979)
[7] E. Eisenriegler, K. Kremer, and K. Binder, J. Chem. Phys. **77**, 6296 (1982)
[8] H. Meiroitch and S. Livne, J. Chem. Phys. **88**, 4507 (1988)
[9] P. Y. Lai, Phys. Rev. E **49**, 5420 (1994)
[10] R. Hegger and P. Grassberger, J. Phys. A: Math. Gen. **27**, 4069 (1994)
[11] H. W. Diehl and M. Shpot, Nucl. Phys. B **528**, 595 (1998)
[12] J. De Joannis, R. R. Ballamudi, C..-W. Park, J. Thomatos and I,. A. Bitsanis, Europhys. Lett. **56**, 200 (2001)
[13] S. Metzger, M. Müller, K. Binder, and J. Baschnagel, Macromol. Theory & Simul. **11**, 985 (2002)
[14] R. R. Netz and D. Andelman, Phys. Rep. **380**, 1 (2003)

[15] R. Descas, J.-U. Sommer, and A. Blumen, J. Chem. Phys. **120**, 8831 (2004)
[16] P. Grassberger, J. Phys. A:Math. Gen. **38**, 323 (2005)
[17] J. Krawczyk, A. L. Owzcarek, T. Prellberg, and A. Rechnitzer, Europhys. Lett. **70**, 726 (2005)
[18] K. Binder, W. Paul, T. Strauch, F. Rampf, V. A. Ivanov, and J. Luettmer-Strathmann, J. Phys.: Condens. Matter **20**, 494215 (2008)
[19] S. Bhattacharya, A. Milchev, V. G. Rostiashvili, and T. A. Vilgis, Eur. Phys. J. E**29**, 285 (2009)
[20] L. I. Klushin, A. A. Polotsky, H.-P. Hsu, D. A. Markelow, K. Binder, and A. M. Skvortsov, Phys. Rev. E**87**,022604 (2013)
[21] H.-P. Hsu and K. Binder, Macromolecules **46**, 2496 (2013)
[22] P. J. Flory, *Statistical Mechanics of Chain Molecules* (Interscience, New York, 1969)
[23] P. G. de Gennes, *Scaling Concepts in Polymer Physics* (Cornell Univ. Press, Ithaca, 1998)
[24] J. G. Le Guillou and J. Zinn-Justin, Phys. Rev. B**21**, 3976 (1980)
[25] A. D. Sokal, in *Monte Carlo and Molecular Dynamics in Simulations in Polymer Science*(K. Binder, ed) Chapter 2 (Oxford Univ. Press, New York, 1995)
[26] N. Clisby, Phys. Rev. Lett. **104**, 055702 (2010)
[27] R. Tijssen, H.A. Billiet, and P.I. Schoenmakers, J. Chromatogr. Sci. **122**, 185 (1976)
[28] R.K. Gilpin, J. Chromatogr. Sci. **22**, 371 (1984)
[29] K.A. Dill, J. Naghidazeh, and A. Marqusee, Annu. Rev. Phys. Chem. **39**, 425 (1988)
[30] J.G. Dorsey and K.A. Dill, Chem. Rev. **89**, 931 (1989)
[31] S.J. Andersen and K.S. Bird, Progr. Colloid Polym. Sci. **82**, 52 (1990)
[32] M.R. Böhmer, L.L. Koopal, and R. Tijssen, J. Phys. Chem. **95**, 6285 (1991)
[33] H. Pasch and B. Trathnigg, *High Performance Liquid Cromatography of Polymers* (Springer, Berlin, 1999) **XIV**, p. 1-16
[34] A. Milchev and K. Binder, J. Chem. Phys. **136**, 194901 (2012)
[35] A. Halperin, M. Tirrell and T. P. Lodge, Adv. Polym. Sci **100**, 31 (1992)
[36] K. Binder and A. Milchev, *J. Polym. Sci., Part B: Polym. Phys.* **50**, 1515 (2012), and references therein
[37] A. M. Skvortsov, L. I. Klushin, A. A. Polotsky, and K. Binder, EPL **104**, 18009 (2013)
[38] A. A. Gorbunov and A. M. Skvortsov, Adv. Colloid Int. Sci. **62**, 31-108 (1995)
[39] P. Grassberger, Phys. Rev. E**56**, 3682 (1997))
[40] H.-P. Hsu and P. Grassberger, J. Stat. Phys. **144**, 597 (2011)
[41] L. Schäfer, *Excluded Volume Effects in Polymer Solutions as Explained by the Renormalization Group* (Springer, Berlin, 1997)
[42] S. Alexander, J. Phys. (Paris) **38**, 983 (1977)
[43] P.-G. de Gennes, Macromolecules **13**, 1069 (1980)
[44] A. Yu. Grosberg and A.R. Khokhlov, *Statistical Physics of Macromolecules* (AIP Press, New York, 1994)
[45] J. Paturej, A. Milchev, S.A. Egorov and K. Binder, Soft Matter **9**, 10522 (2013)
[46] A. Milchev, S.A. Egorov and K. Binder, J. Chem. Phys. **132**, 184905 (2010)
[47] G.S. Grest, K. Kremer and T.A. Witten, *Macromolecules* **20**, 1376 (1987).
[48] G.S. Grest and K. Kremer, *Phys. Rev. A* **33**, 3628 (1986).
[49] M. Murat and G.S. Grest, *Macromolecules* **29**, 1278 (1996).
[50] F.A.M. Leermakers and J.M.H.M. Scheutjens, J. Chem. Phys. **89**, 2264 (1988); *ibid* **89**, 6912 (1988)
[51] O.A. Evers, J.M.H.M. Scheutjens, and G.J. Fleer, Macromolecules **23**, 5221 (1990)
[52] S. A. Egorov, J. Chem. Phys. **129**, 064901 (2008).
[53] F. LoVerso, S. A. Egorov, A. Milchev, and K. Binder, J. Chem. Phys. **133**, 184901 (2010).